JPET Fast Forward. Published on May 10, 2013 as DOI: 10.1124/jpet.113.203653
This article has not been copyedited and formatted. The final version may differ from this version.

JPET #203653

Estrous Cycle Regulation of Extrasynaptic δ-Containing $GABA_A$ Receptor-mediated Tonic Inhibition and Limbic Epileptogenesis in Mice

Xin Wu, Omkaram Gangisetty, Chase Matthew Carver and Doodipala Samba Reddy*

Department of Neuroscience and Experimental Therapeutics, College of Medicine, Texas A&M University Health Science Center (X.W., O.G., C.M.C. and D.S.R.), Bryan, TX 77807, USA

JPET Fast Forward. Published on May 10, 2013 as DOI: 10.1124/jpet.113.203653
This article has not been copyedited and formatted. The final version may differ from this version.

Running Title Page

Running title: Estrous Cycle Regulation of Tonic Inhibition and Epileptogenesis

Address of corresponding author:

D. Samba Reddy, Ph.D., R.Ph.
Professor
Department of Neuroscience and Experimental Therapeutics
College of Medicine
Texas A&M University Health Science Center
1005 Medical Research and Education Building
8447 State Highway 47, Bryan, TX 77807-3260
Phone: 979-436-0324
E-mail: reddy@medicine.tamhsc.edu

Manuscript statistics:
Number of pages = 35
Figures = 8
References = 70
Words in Abstract = 250
Words in Introduction = 565
Words in Discussion = 1733

ABBREVIATIONS*:*
AD, afterdischarge; AP, allopregnanolone; CA1PCs: CA1 pyramidal cells; DGGCs: dentate gyrus granule cells; GABA, γ-aminobutyric acid; G_{rms}: root-mean-square noise conductance; G_{tonic}: mean peak tonic conductance; NS: neurosteroid; PRKO: progesterone receptor knockout.

Recommended section: **Neuropharmacology**

JPET Fast Forward. Published on May 10, 2013 as DOI: 10.1124/jpet.113.203653
This article has not been copyedited and formatted. The final version may differ from this version.

Abstract

The ovarian cycle affects susceptibility to behavioral and neurological conditions. The molecular mechanisms underlying these changes are poorly understood. Deficits in cyclical fluctuations in steroid hormones and receptor plasticity play a central role in physiological and pathophysiological menstrual conditions. It has been suggested that synaptic $GABA_A$ receptors mediate phasic inhibition in the hippocampus and extrasynaptic receptors mediate tonic inhibition in the dentate gyrus. In this study, we report a novel role of extrasynaptic, δ-containing $GABA_A$ receptors as crucial mediators of the estrous cycle-related changes in neuronal excitability in mice, with hippocampus subfield specificity. In molecular and immunofluorescence studies, there was significant increase in δ-subunit, but not α4- and γ2-subunits, in the dentate gyrus during diestrus stage. However, δ-subunit upregulation was not evident in the CA1 region. The δ-subunit expression was undiminished by age, ovariectomy, and in mice lacking progesterone receptors, but was significantly reduced by finasteride, a neurosteroid synthesis inhibitor. Electrophysiological studies confirmed greater potentiation of GABA currents by progesterone-derived neurosteroid allopregnanolone in dissociated dentate gyrus granule cells in diestrus than in CA1 pyramidal cells. The baseline conductance and allopregnanolone potentiation of tonic currents in dentate granule cells from hippocampal slices were higher than in CA1 pyramidal cells. In behavioral studies, susceptibility to hippocampus kindling epileptogenesis was lower in mice during diestrus stage. These results demonstrate the estrous cycle-related plasticity of neurosteroid-sensitive, δ-containing $GABA_A$ receptors that mediate tonic inhibition and seizure susceptibility. These findings may provide novel insight on molecular cascades of menstrual disorders like catamenial epilepsy, premenstrual syndrome and migraine.

JPET Fast Forward. Published on May 10, 2013 as DOI: 10.1124/jpet.113.203653
This article has not been copyedited and formatted. The final version may differ from this version.

Introduction

The menstrual cycle influences many brain conditions. Estradiol is secreted in the second half of the follicular phase and increases to a peak at midcycle, while progesterone is elevated during the luteal phase and declines before menstruation begins (Reddy, 2009; 2013). Fluctuations in steroid hormones, deficits in their cyclical availability, and receptor plasticity play a central role in susceptibility to menstrual conditions such as premenstrual syndrome, migraine, and catamenial epilepsy (Backstrom et al., 2003; Reddy, 2009). Catamenial epilepsy is characterized by seizures that cluster most often during the perimenstrual or periovulatory period when progesterone levels are low (Herzog and Frye, 2003; Herzog et al., 2004; 2011; Reddy et al., 2012). However, the molecular mechanisms underlying these changes remain unclear.

Progesterone is a precursor for the synthesis of neurosteroids such as allopregnanolone (AP) in the brain (Reddy and Mohan, 2011). These neurosteroids are increased in parallel to their precursor progesterone during the menstrual cycle (Tuveri et al., 2008). Progesterone and neurosteroids have anxiolytic, anticonvulsant, and neuroprotective properties (Reddy, 2004; 2005) and have been shown to play a significant role in epilepsy, anxiety, and depression (Smith et al., 1998b; Reddy, 2003; van Broekhoven and Verkes, 2003; Reddy and Jian, 2010). Neurosteroids rapidly alter neuronal excitability through direct interaction with $GABA_A$ receptors ($GABA_ARs$) (Hosie et al., 2007). $GABA_ARs$ are composed of five subunits from several classes (α_{1-6}, $\beta_{1-4,}$ γ_{1-3},δ,ε,θ, ρ_{1-3}). The major isoforms consist of 2α, 2β, and 1γ- or 2α, 2β, and 1δ-subunits. It has been reported that synaptic (mainly γ2-containing) receptors mediate phasic inhibition in the hippocampus and extrasynaptic (mainly δ-containing) receptors mediate tonic inhibition in the dentate gyrus. Neurosteroids act on both synaptic and extrasynaptic receptors as positive $GABA_AR$ allosteric modulators (Reddy, 2010; Uusi-Oukari and Korpi, 2010), but cause large effects on δ-containing extrasynaptic $GABA_ARs$, which are persistently activated by ambient GABA (Belelli et al., 2002; Stell et al., 2003). The resulting tonic conductance generates shunting inhibition that controls network excitability and behavior.

The ovarian cycle modulates behavior and seizure susceptibility (Reddy and Kulkarni, 1999; Molina-Hernandez et al., 2001; Maguire et al., 2005; 2009). Changes in neuronal excitability occur during changes in reproductive status such as puberty, pregnancy or menopause. During puberty, the level of steroid hormone increases and behavioral changes begins. Because neurosteroids influence inhibition, behavioral and learning deficits observed during puberty are linked to changes in δ-containing $GABA_ARs$ (Shen et al., 2007; 2010). Ovarian cycle-linked fluctuations in progesterone and

neurosteroids have been proposed to alter $GABA_AR$-mediated tonic inhibition (Maguire et al., 2005; Gangisetty and Reddy, 2010; Reddy et al., 2012). However, there is little information on molecular mechanisms by which $GABA_AR$ subunit composition and function in hippocampus subfields is regulated by the ovarian cycle. It is poorly understood how progesterone-derived neurosteroid AP modulates neuroplasticity and epileptogenesis during ovarian cycle.

In this study, we determined the estrous cycle-related changes in $GABA_AR$ δ-subunit expression and tonic inhibition in the hippocampus subfields along with susceptibility to epileptogenesis in female mice. To simulate the luteal (high progesterone) and follicular (low progesterone) phases, we focused on diestrus (high progesterone) and estrus (low progesterone) stages that exhibit a comparable hormonal milieu with the human ovarian cycle. Our results demonstrate novel estrous cycle-related changes of δ-containing $GABA_ARs$ expressions in different hippocampal subfields, and $GABA_ARs$ δ-subunit-mediated tonic inhibition and seizure susceptibility, such as that which occur in catamenial epilepsy. These findings are also relevant to premenstrual syndrome and migraine in women.

JPET Fast Forward. Published on May 10, 2013 as DOI: 10.1124/jpet.113.203653
This article has not been copyedited and formatted. The final version may differ from this version.

Materials and Methods

Animals and Estrous Cycle Studies

Animals. Female adult (3-5 months-old) wild-type (WT) and progesterone receptor knockout (PRKO) mice weighing 25-30 g were used in the study. The development of the PRKO mouse strain and genotyping procedures have been described previously (Lydon et al., 1995; Reddy et al., 2004). These mice were maintained on a hybrid C57BL6/129SV background. Basal levels of progesterone in serum were reported to be similar in the WT and PRKO groups (Chappell et al., 1997). The mice were housed in an environmentally controlled animal facility under a 12 h/12 h light/dark cycle and allowed free access to food and water, except during the experimental sessions. Genotype was confirmed by PCR using mouse tail genomic DNA (Reddy et al., 2005). Young, adult mice with regular cycles and aged mice (18 months old) that were acyclic were used in the study. Ovariectomized, young, adult mice were used for experiments 2 weeks following the surgical procedure. All procedures were performed in strict compliance with the guidelines of National Institutes of Health Guide for the Care and Use of Laboratory Animals under a protocol approved by the university's Institutional Animal Care and Use Committee.

Determination of Estrous Cycle and Plasma Progesterone Levels. Mice exhibit a 6-day ovarian cycle/estrous cycle, which is subdivided into four stages that are associated with distinct hormonal milieu. Estrous cycle was determined by microscopic examination of vaginal smears with eosin staining (Maguire et al., 2005). Diestrus stage was characterized by the presence of many leukocytes. Proestrus stage was determined by largely small round nucleated epithelial cells. Estrus stage was confirmed by large anucleated cornified squamous epithelial cells. Metestrus stage was represented by both leukocytes and epithelial cells (Fig.1). Estrus and diestrus stages of the cycle were chosen for further experiments. For studies of progesterone assay, mice were anesthetized with isoflurane and 0.5 ml carotid blood was collected in heparinized tubes. The plasma was separated by centrifugation at 12,000 rpm for 10 min at 4°C. Plasma concentrations of progesterone were analyzed by an immunoassay. The detection limit of the assay was <0.2 ng/ml. In order to simulate the luteal (high progesterone) and follicular (low progesterone) phases, we focused on diestrus (high P) and estrus (low P) stages that exhibit comparable hormonal levels to human menstrual cycle.

Molecular and Cellular Studies

TaqMan Real-Time PCR. The $GABA_AR$ subunit mRNA expression was determined by the TaqMan real-time PCR assay as described previously (Gangisetty and Reddy, 2009). The

JPET Fast Forward. Published on May 10, 2013 as DOI: 10.1124/jpet.113.203653
This article has not been copyedited and formatted. The final version may differ from this version.

hippocampus was rapidly dissected for total RNA extraction by using a Trizol reagent (Invitrogen Inc., Carlsbad, CA). cDNA was prepared using the Superscript II first-strand cDNA synthesis kit (Invitrogen Inc., Carlsbad, CA). The PCR primers and TaqMan probe sequences specific for $GABA_AR$ subunits, such as α4 and δ-subunits, and GAPDH genes were designed and optimized for real-time PCR analysis using the Primer Express software (Applied Biosystems Inc., Foster City, CA) (Gangisetty and Reddy, 2009). TaqMan PCR reactions were carried out in an AB 7500 fast real-time system (Applied Biosystems). Real-time PCR was performed with TaqMan Universal PCR Master Mix (Applied Biosystems), which contained AmpliTaq Gold DNA Polymerase, AmpErase, UNG, dNTPs with dUTP, and optimized buffer components. Briefly, each sample was run in triplicate design and each 25-µl reaction mixture consists of 12.5-µl TaqMan Universal PCR Master mix, 400 nM primers, and 300 nM TaqMan probe for each targeted genes as described previously (Gangisetty and Reddy, 2009). The real-time PCR run consisted first of one cycle of 50 °C for 2 min (AmpErase activation), then one cycle of 95 °C for 10 min (Taq activation), and 50 cycles of 95 °C for 15 s and 60 °C for 1 min (denaturation, annealing and extension). The $GABA_AR$ subunit mRNA expression was normalized to GAPDH expression as a percent change in the same samples.

Western Blot Analysis. Western blot analysis of $GABA_AR$ δ-subunits was performed with modification of published protocol (Maguire et al., 2005; Gangisetty and Reddy, 2010). Membrane protein (50 µg) from hippocampus was loaded on to 12% Tris-HCl gel (Bio-Rad) and subjected to electrophoresis at 75 V for 3 h under denaturing conditions. The proteins were transferred to polyvinylidene fluoride membrane (Bio-Rad) and then blocked in 5% nonfat milk at room temperature for 1 h. Membranes were then incubated with a rabbit polyclonal antibody specific for $GABA_AR$ δ-subunits (1:500. PhosphoSolutions, Aurora, CO), mouse monoclonal β-actin antibody (1:1000 dilution, Santa Cruz Biotechnology, Santa Cruz, CA) at 4 °C for overnight. Membranes were then washed three times with 1X Tris-buffered saline and Tween 20 at room temperature for 20 min. The blots were then incubated with anti-rabbit antibody (1:2500) conjugated to horseradish peroxidase for 1 h at room temperature. Blots were washed three times for 20 min in 1X TBST. Immunoreactive $GABA_AR$ δ-subunit bands (52 kDa) were detected using enhanced chemiluminiscent reagents (Pierce), and then membranes were stripped and re-probed with the mouse monoclonal antibody for β-actin. Protein bands were quantified using alpha imager software (Alpha Innotech, San Leandro, CA, USA). β-Actin was used as internal control. Changes in δ-subunit expression was expressed as percent change from control values.

JPET Fast Forward. Published on May 10, 2013 as DOI: 10.1124/jpet.113.203653
This article has not been copyedited and formatted. The final version may differ from this version.

Immunocytochemistry and Confocal Microscopy. The δ-subunit distribution in the hippocampal neurons was determined by immunocytochemistry and confocal microscopy as per the methodology published previously with slight modifications (Mangan et al., 2005; Wu et al., 2010; Tangney et al., 2013). A suspension of freshly dissociated hippocampal CA1 pyramidal cells (CA1PCs) and dentate gyrus granule cells (DGGCs) from adult female mice in the diestrus and estrus stages was plated onto a thin glass bottom dishes for 2 h. The cells were fixed with 4% paraformaldehyde for 15 min followed by four washes in phosphate-buffered saline (PBS) containing 0.1 M glycine. Cells were permeabilized with ice-cold methanol at 4 °C for 1 min followed again by four rinses with PBS solution. Cells were then incubated with blocking solution containing 1% bovine serum albumin (Vector Laboratories, UK), 2.5% normal goat serum, 5% 20x saline-sodium citrate (Sigma-Aldrich, St. Louis, MO) and 0.1% Triton X-100 for 1 h. After the blocking phase, the cells were incubated with the primary rabbit $GABA_AR$ δ-subunit antibody (N-Terminus, 1:100, PhosphoSolutions) or control rabbit IgG (1:100, Santa Cruz Biotechnologies) for 1 h at room temperature. Cells were rinsed with PBS solution and then incubated with Alexa Fluor® 555 labeled secondary antibody of goat-anti-rabbit IgG (1:200, Molecular Probes, Invitrogen) for 1 h in the dark. Cells were washed with PBS solution four times, treated with 1-2 drops of ProLong AntiFade (Molecular Probes, Invitrogen, Inc.) and covered with coverslip. Serial image sections through focus with step size of 0.1-0.3 µm thickness were collected and analyzed using Nikon confocal microscope with NIS-Elements software suite (Nikon Instruments, Inc). The normalized mean intensity was calculated from the ratio from the mean intensity of $GABA_AR$ δ-subunits minus background to the mean density of control Ab minus background. The normalized integrated mean intensity was used to compare density from different experimental groups.

Electrophysiological Studies

Hippocampal Slices Preparation. Transverse slices (300-400 µm thickness) of hippocampus were prepared using standard techniques from adult female mice in the diestrus and estrus stages. Mice were anesthetized with isoflurane and brains were excised rapidly. The brains were placed in cold (4 °C) artificial cerebrospinal fluid (ACSF) buffer containing 0.3 mM kynurenic acid (Tocris Bioscience, MN). ACSF buffer was composed of (in mM): 126 NaCl, 3 KCl, 2 $CaCl_2$, 2 $MgCl_2$, 26 $NaHCO_3$, 1.25 NaH_2PO_4, 11 glucose (pH adjusted to 7.35-7.40 by gassed with 95% O_2 – 5% CO_2. Osmolarity, 305–315 mOsm/kg). Several hippocampus slices were cut with a Vibratome (model 1500 with 900 Refrigeration System; Leica Microsystems, Inc., Bannockburn, IL). Hippocampus were dissociated from the microdisected subfield tissues CA1, CA3 and dentate gyrus (DG), respectively. The tissue samples collected were rapidly frozen for RNA and protein extractions. For

JPET Fast Forward. Published on May 10, 2013 as DOI: 10.1124/jpet.113.203653
This article has not been copyedited and formatted. The final version may differ from this version.

electrophysiology and immunocytochemistry studies, the microdisected subfield hippocampal slices were equilibrated in ACSF at 24°C on a mesh surface in a small beaker in a water bath (Thermo-Fisher Scientific, Waltham, MA) continuously bubbled with oxygen (95% O_2 and 5% CO_2).

Dissociation of Neurons. The dissociation of hippocampal CA1PCs or DGGCs were prepared by the standard dissociation technique described previously (Kay and Wong, 1986; Reddy and Jian, 2010) from adult female mice in the diestrus and estrus stages. The hippocampal pieces of the CA1 or DG region were microdisected carefully under the microscope (model SMZ 647; Nikon, Tokyo, Japan) and incubated in ACSF for 1 h at 24°C. The isolated slices were transferred into an enzymatic solution consisting of ACSF with protease XXIII (3 mg/ml, Sigma-Aldrich, St. Louis, MO). The slices were then incubated for precisely 23 to 25 min at 24°C. The remaining slices were rinsed twice with ACSF and gently triturated through three different sizes of fire-polished Pasteur pipettes to release single cells. For this step, three fire-polished Pasteur pipettes with increasingly smaller tips were used. For each batch, slices were triturated five or six times with each pipette with approximately 1 ml of ACSF in it. Then, the solution was allowed 1 min for the tissue to settle down, and the suspension of freshly dispersed cells were carefully plated onto the recording chamber for electrophysiology and immunocytochemistry experiments (Warner Instruments, Hamden, CT).

Recording of GABA-evoked Currents. Electrophysiological recordings were performed in the whole-cell patch-clamp configuration (Reddy and Jian, 2010). All electrophysiological experiments were performed at 22-24 °C. The recording chamber was fixed into the stage of an inverted microscope with phase-contrast and differential interference contrast optics (model IX71; Olympus, Tokyo, Japan). The physiological bath solution for isolated single cell recording had the following composition (PSS, in mM): 140 NaCl, 3 KCl, 10 HEPES, 2 $MgCl_2$, 2 $CaCl_2$, and 16 glucose (pH adjusted to 7.4 with NaOH, osmolarity, 315–325 mOsm/kg). Cells were visualized and images were acquired through video camera CCD-100 (Dage-MTI, Michigan City, IN) with FlashBus Spectrim 1.2 software (Pelco, Clovis, CA). Recording pipettes were pulled from capillary glass tubes (King Precision Glass, Claremont, CA) using a P-97 Flaming-Brown horizontal puller (Sutter Instrument Company, Novato, CA). The pipette tip resistances were 2 to 4 MΩ for single cell recording and 4 to 6 MΩ for slices recording. The pipettes were dipped for 2–3 s in a Cs^+ pipette solution (high Cs^+ for isolated single cell and slices recording) containing (in mM) 124 CsCl, 20 tetraethylammonium, 2 $MgCl_2$, 10 EGTA, 10 HEPES, 0.1 GTP, 4 ATP (pH adjust to 7.2 with CsOH, osmolarity, 295–305 mOsm/kg). Pipettes were back-filled with the same solution. Currents were recorded by using an Axopatch 200B amplifier (Molecular Devices, Sunnyvale, CA). The membrane capacitance, series resistance, and input resistance of the recordings were monitored by applying a 5-mV (100-ms)

JPET Fast Forward. Published on May 10, 2013 as DOI: 10.1124/jpet.113.203653
This article has not been copyedited and formatted. The final version may differ from this version.

depolarizing voltage step from a holding potential of -70 mV. Signals were low-pass filtered at 1 kHz and digitized at 2 kHz with Digidata 1440A system. The current values were normalized to cell capacitance (an index of cell size) and expressed as current density (pA/pF). For whole cell current from isolated single cells, fractional potentiation produced by test drugs was calculated as I_{NS}/I_{GABA}, where I_{GABA} was the response of peak amplitude at the application of GABA (3 μM) and I_{NS} is the response of peak amplitude at the co-application of GABA and the neurosteroid AP (10 nM to 1 μM). For fast application of test drugs, the perfusion pipette was positioned <100 μm away from the cell in the dish. GABA, allopregnanolone, and $GABA_AR$ competitive antagonist bicuculline (BIC, 10 μM) were applied using a multi-channel perfusion system (Automate Scientific, Berkeley, CA).

Tonic Current Recording and Analysis. The $GABA_AR$ mediated tonic current recording and analysis were made as described previously (Mtchedlishvili and Kapur, 2006). Hippocampal slices (300 μm) for were maintained in continuously oxygenated ASCF at 32°C in a holding chamber for 60 min, and then back to room temperature in a recording chamber. Hippocampal CA1PCs and DGGCs were visually identified using an Olympus BX51 microscope equipped with a 40x□water-immersion objective, infrared-differential interference contrast optics, and video camera (Kay and Wong, 1986). Tonic currents of $GABA_ARs$ were recorded in the presence of tetrodotoxin (TTX, 0.5 μM, Na^+ channel blocker, Calbiochem), d(-)2-amino-5-phosphonovaleric acid (APV, 40 μM, N-methyl-D-aspartate channel blocker, Sigma), and 6,7-dinitroquinoxaline-2,3-dione (DNQX, 10 μM, non-N-methyl-D-aspartate glutamate receptor blocker) and confirmed by $GABA_AR$ inhibitor BIC (10 μM). Off-line analysis of tonic currents were analyzed with Mini-Analysis software (Synaptosoft, Leonia, NJ) (Mtchedlishvili and Kapur, 2006). To study the tonic inhibition, transient events were manually removed from the current trace, so that it consisted only of membrane current at the voltage-clamp mode. To account for cell-to-cell variability, the tonic current was expressed as a conductance (G (pS) = tonic current / membrane potential) normalized to membrane capacitance (pS/pF). Averaged amplitude of tonic current conductance ($G_{tonic,}$ pS/pF) and root-mean-square noise amplitude ($G_{rms,}$ pS/pF) were measured (Fig. 6). G_{tonic} is the current conductance from the difference in holding potential (HP = - 60 mV) before and after application of bicuculline. G_{rms} is the noise conductance from chloride ions passing through the opened channels and in proportion to the chloride driving force. G_{tonic} was measured and averaged in 100 ms each epoch with 1 sec interval between epochs for 30 epochs. The measurements were taken 30 s before and 3 min after application of a drug. G_{rms} was studied in 50 ms each epoch with 500 ms interval between epochs for 30 epochs before and after drug application in each cell. To assess the effect of a drug on G_{rms} in an individual neuron, the distribution of G_{rms} in 30 epochs before the application of a drug (during the baseline period) was

JPET Fast Forward. Published on May 10, 2013 as DOI: 10.1124/jpet.113.203653
This article has not been copyedited and formatted. The final version may differ from this version.

compared with that after drug application by means of Kolmogorov-Smirnov test. To compare data obtained from a group of neurons, G_{rms} values in individual epochs before and after drug application were averaged.

Behavioral Studies

Hippocampus Kindling Epileptogenesis. The rapid kindling model of epileptogenesis was utilized for assessment of seizure susceptibility over the estrous cycle. Rapid kindling allows accelerated evaluation of experimental manipulations during the progression of epilepsy induction (Lothman and Williamson, 1993; Reddy and Mohan, 2011). The rapid kindling procedure was similar to the conventional kindling with daily stimulations except that stimulations were applied every 30 min until mice exhibited consistent stage 5 seizures. This procedure has been used extensively as a model of compressed epileptogenesis. A mild focal, nonconvulsant electrical stimulus to the hippocampus on a repeated basis leads to development of a kindled state exhibiting electrographic and behavioral seizures. In mouse kindling, the focal EEG afterdischarge models complex partial seizures, while the behavioral motor seizure stages 4/5 models generalized seizures.

Electrode implantation and stimulation procedures for mouse hippocampus kindling were performed as described previously (Reddy and Mohan, 2011). Mice were anesthetized by an intraperitoneal injection of ketamine (100 mg/kg. i.p.) and xylazine (20 mg/kg, i.p.). A stimulation-recording bipolar electrode (model MS303/1; Plastic One, Roanoke, VA) was stereotaxically implanted in the right ventral hippocampus (2.9 mm posterior, 3.0 mm lateral, and 3.0 mm below dura) using the Franklin and Paxinos atlas (1997). The electrode was anchored with dental acrylic to three small screws placed in the skull. After a postoperative recovery period of at least 1 week, the electrographic afterdischarge (AD) threshold was determined by an application of 1 ms duration of biphasic rectangular pulses at 60 Hz for 1 s, beginning at 25 μA by using an isolated pulse stimulator (A-M Systems, Sequim, WA). AD duration was the total duration of hippocampus electrographic spike activity (amplitude > 2 x baseline) occurring in a rhythmic pattern at a frequency >1 Hz. Additional stimulations increasing in increments of 25 μA were given at 5 min intervals until an electrographic AD duration lasting at least 5 s was detected using the digital EEG system (Astro-Med, West Warwick, RI). Mice were stimulated at 125% AD threshold (1 ms duration pulse, 60 Hz frequency for 1 s) at 30-min intervals until they showed stage 5 seizure, which is considered the fully-kindled state (Reddy and Mohan, 2011). Stimulations were delivered every 30 min until stage 5 seizures were elicited on 3 consecutive trials. The electrographic activity and AD duration were acquired from the hippocampal electrode using Axoscope 8.0 software with Digidata 1322A interface (Molecular Devices, Sunnyvale, CA) through a Grass CP511 preamplifier (Astro-Med, West Warwick, RI). Behavioral seizures were

JPET Fast Forward. Published on May 10, 2013 as DOI: 10.1124/jpet.113.203653
This article has not been copyedited and formatted. The final version may differ from this version.

rated according to Racine's scale (Racine, 1972) as modified for the mouse: stage 0, no response or behavior arrest; stage 1, chewing or facial twitches; stage 2, chewing and head nodding; stage 3, forelimb clonus; stage 4, bilateral forelimb clonus and rearing; stage 5, falling. Kindling is a permanent phenomenon and an intense seizure can be elicited weeks or months after kindling development. Mice with electrode implanted but non-stimulated were used as sham controls. To determine the effect of AP on kindling progression, animals were subcutaneously injected with AP (3 mg/kg. s.c.) 15-min before kindling sessions. Control animals were injected similarly with vehicle (15% cyclodextrin solution). During each stimulation session, the behavioral seizure score and the AD duration were noted. Rate of kindling development, that is numbers of stimulation required to induce stage 5 seizures, was determined in mice at estrus and diestrus stages with or without AP treatment. Cumulative AD duration was calculated as an index of total seizure activity for reaching stage 5 seizure. At the end of the study, mice were anesthetized and perfused transcardially with paraformaldehyde for Nissl staining to verify the electrode placement.

Data Analysis. Group data was expressed as mean ± SEM. The $GABA_AR$ subunit expression was analyzed based on the relative quantification approach as described previously (Gangisetty and Reddy, 2010). For electrophysiology, we used data only from cells in which stable gigaseals were maintained. In most analyses, the raw current value was normalized to cell capacitance (an index of cell size) and expressed as current density (pA/pF) or current conductance (pS/pF). Statistical comparisons were performed with repeated-measures analysis of variance followed by post hoc tests, or with an independent two-tail *t*- test, as appropriate. Comparison of the mean percentage inhibition of seizure stage in animals was made by Wilcoxon signed ranks test. Significant differences in the rate of kindling and AD durations between groups were assessed by repeated measures ANOVA, or one-way ANOVA followed by Dunnett's *t*-test. Differences were considered statistically significant at $P< 0.05$.

Drugs and Treatments. Stock solutions of finasteride and AP (Steraloids Inc., Newport, RI) and other drugs for injection were made in 15% β-cyclodextrin in saline, and additional dilutions were made using sterile saline. Drug solutions were administered subcutaneously or intraperitoneally in a volume equaling 1% of the animal's body weight. β-Cyclodextrin and other reagents were procured from Sigma-Aldrich (St. Louis, MO) unless otherwise noted.

JPET Fast Forward. Published on May 10, 2013 as DOI: 10.1124/jpet.113.203653
This article has not been copyedited and formatted. The final version may differ from this version.

Results

Determination of the Estrous Cycle and Progesterone Levels in Mice. To model the menstrual cycle-related changes in ovarian hormones, we investigated the mouse estrous cycle. Different stages of the cycle were determined by microscopic examination of vaginal smears (Fig. 1A) and by estimating plasma progesterone levels (Fig. 1B). The average length of the cycle was 6 days. Among the four different stages, diestrus 1 is considered similar to the luteal phase and estrus is similar to the perimenstrual phase of the menstrual cycle (Fig. 1A). Plasma progesterone levels were significantly higher in diestrus 1 (10.3±2.0 ng/ml) relative to estrus (2.5±0.3 ng/ml) (Fig. 1B). Diestrus 2 is not associated with significant increase in the levels of progesterone. For the purposes of this paper, diestrus 1 will be referred to simply as diestrus. These two stages of the estrous cycle were selected for further characterization.

Cyclical Alterations in $GABA_A$ Receptor Subunit Expression During the Estrous Cycle. To determine the cyclical changes in $GABA_AR$ subunit plasticity in the hippocampus, we carried out TaqMan real-time PCR assay and western blot analysis of receptor subunit expression in the hippocampus subfields of the CA1, CA3, and DG regions. The expressions of $GABA_AR$ α1-subunit mRNA in CA1 and DG, $GABA_AR$ α2- and δ-subunits mRNA in CA3 and DG showed significant increase in diestrus as compared to estrus (Fig. 2). Quantification of δ-subunit mRNA copy number revealed a considerably greater expression within DG compared to the other hippocampus subfields (Fig. 2F). There was an increase in the expression of δ-subunit in CA1 pyramidal layer, but it did not reach statistical significance (Fig. 2A). In addition, there were no significant changes in the expression levels of $GABA_AR$ α4- and γ2-subunits in any of the hippocampus subfields (Fig. 2). To determine whether changes in δ-subunit mRNA levels are translated to increase in neuronal δ-subunit protein, we determined the δ protein levels from DG of estrus and diestrus stages. Western blot analysis indicated significant increase in total δ-subunit protein expression in diestrus as compared to estrus (Fig. 2D and 2E).

To confirm the presence of $GABA_AR$ δ-subunits in neurons of hippocampus, the single cell distribution of δ-subunit was determined by fluorescent immunocytochemistry using a primary antibody specific for the δ-subunit. The staining with δ-subunit antibody showed broad distribution on the soma, axon, and dendritic regions of freshly dissociated CA1PCs and DGGCs acquired from estrus or diestrus (Fig. 3A). The normalized δ-subunit staining intensity, expressed as percentage change in fluorescence intensity relative to the value for control IgG was 2.23-fold greater in DGGCs

JPET Fast Forward. Published on May 10, 2013 as DOI: 10.1124/jpet.113.203653
This article has not been copyedited and formatted. The final version may differ from this version.

in diestrus as compared to estrus (Fig. 3B, $p<0.05$). The δ-subunit protein was concentrated on cell membrane as shown in images from X-Z and Y-Z axes obtained from confocal microscopy (Fig. 3C). Our data was consistent with previous study that AP-induced increase in δ-subunit expression was most likely via insertion of receptors in the cell membrane (Kuver et al., 2012). Taken together, these results demonstrate dynamic variations in $GABA_AR$ subunits composition and especially δ-subunit over the estrous cycle, whereby elevated progesterone levels in diestrus correlated with increased $GABA_AR$ δ-subunit expression.

Influence of Age and Ovariectomy on the $GABA_A$ Receptor δ-Subunit Expression. We next investigated whether aging and ovarian hormones alter $GABA_A$ receptor δ-subunit expression in the hippocampus. TaqMan RT-PCR analysis of δ-subunit expression was carried out in the hippocampus subfields CA1, CA3 and DG regions in ovariectomized and aged mice in comparison with young adult females. It has been reported that ovariectomized mice and aged, acyclic mice show compensative progesterone production from other places such as adrenal cortex (Lu et al., 1979; Steger and Peluso, 1982). In aged, acyclic, female mice, $GABA_AR$ δ-subunit mRNA expression was significantly increased in CA3 and DG regions as compared to young, adult mice in estrus stages. There was no significant difference in the expression of $GABA_AR$ δ-subunit in CA1 regions between young and aged mice (Fig. 4A). There was a significant increase in the expression of δ-subunit in DG from ovariectomized mice compared to estrus mice. However, there was no significant difference in the expression of δ-subunit from ovariectomized mice compared to diestrus mice in the CA1, CA3 and DG regions (Fig. 4A). These results suggest that ovarian cycling is essential and closely associated with regulation of $GABA_AR$ δ-subunit expression.

Role of Progesterone Receptors and Neurosteroids on the $GABA_A$ Receptor δ-Subunit Expression During the Estrous Cycle. We next extended our study to determine a potential mechanistic pathway involving progesterone receptors (PR) and neurosteroids in δ-subunit expression. To determine whether the PR pathway is involved in regulating the δ-subunit expression during the estrous cycle, we utilized female PR knockout (PRKO) mice, which lack both PR-A and PR-B receptor subtypes in the brain (Reddy et al., 2005), as a robust genetic model. We have previously reported that there are no significant differences in $GABA_AR$ α4-subunit expression from wild-type and PRKO mice in the hippocampus (Gangisetty and Reddy, 2010). In PRKO mice, the δ-subunit mRNA expression was significantly increased in CA3 and DG regions as compared with WT estrus stage. There was no significant change of δ-subunit mRNA expression in CA1 region (Fig. 4B).

JPET Fast Forward. Published on May 10, 2013 as DOI: 10.1124/jpet.113.203653
This article has not been copyedited and formatted. The final version may differ from this version.

This result suggests that PRs may not be necessary in the cycle regulation of $GABA_AR$ δ-subunit plasticity.

To explore the relative role of the neurosteroid AP in $GABA_AR$ δ-subunit expression, we employed finasteride, a 5α-reductase inhibitor that blocks the synthesis of progesterone-derived AP (Fig. 4D). After treatment with finasteride (50 mg/kg. i.p.) twice daily for one week, $GABA_AR$ δ-subunit expression was 67% and 38% decreased in control (WT-diestrus) and PRKO mice, respectively (Fig. 4C). These results demonstrate a role of progesterone-derived AP and related neurosteroids, independent of PRs, in regulating $GABA_AR$ δ-subunit expression in the hippocampus.

Cyclical Alterations in Neurosteroid-Sensitive $GABA_A$ Receptor-Mediated Whole-Cell Cl^- Currents During the Estrous Cycle. To study the effect of $GABA_AR$ subunits especially δ-subunit plasticity on receptor function, we used the patch-clamp electrophysiology to assess inhibitory currents in neurons. The effect of allosteric modulators on $GABA_AR$ function is markedly influenced by the presence of the δ-subunit (Maguire et al., 2005; Mtchedlishvili and Kapur, 2006; Rajasekaran et al., 2010). We utilized electrophysiology to confirm δ-subunit-specific pharmacological effects in the dissociated neurons during estrous cycle. In this study, GABA-gated, whole-cell Cl^- currents were recorded in acutely dissociated CA1PCs and DGGCs (Fig.5). Acutely dissociated DGGCs were identified from DG layer as small- and medium-sized neurons with typical oval-shaped soma and single process, and CA1PCs were identified from CA1 layer as typical pyramidal cell body and clear primary apical dendrite (Fig. 5A). Application of GABA (0.1–10000 μM) for 5 second induced an inward currents in a concentration-dependent manner and peaked at 1000 μM in DGGCs from estrus and diestrus (Fig 5A and 5B). First we determined the effect of the estrous cycle-related subunit plasticity of GABA-A receptors on GABA sensitivity. The full GABA concentration-response curves (0.1 – 10000 μM) in DGGCs from estrus and diestrus are illustrated in Fig. 5B. The GABA EC_{50} values were not significant between DGGCs at diestrus (18.4 ± 3.1 μM, n=6) and estrus (20.6 ± 2.9 μM, n=6) animals. Although curves from both cohorts appear similar, the diestrus DGGCs were nearly 12% more sensitive to GABA currents than estrus DGGCs, suggesting the subtle alterations in GABA sensitivity across the estrous cycle. These results are consistent with our previous results of concentration response curves for GABA (0.1–1000 μM)-evoked currents in CA1 neurons (EC_{50} of 15 μM) (Reddy and Jian, 2010).

It has been suggested that the extracellular concentration of GABA in the hippocampus varies from the 2.1 μM to 3.8 μM range (Shin et al., 2002). At 3 μM GABA (~EC_{10}), the channel desensitization is minimal at 30 second intervals between applications (Reddy and Jian, 2010). In

JPET Fast Forward. Published on May 10, 2013 as DOI: 10.1124/jpet.113.203653
This article has not been copyedited and formatted. The final version may differ from this version.

these experiments, we selected a 3 μM concentration of GABA to examine the characteristics of GABA currents that mainly mediate extrasynaptic (δ-subunit) but including synaptic (γ-subunit) $GABA_A$Rs. Application of 3 μM GABA for 5 seconds evoked brief inward currents at a holding potential of -70 mV (Fig. 5A). The inward currents evoked by GABA were completely blocked by the $GABA_A$R antagonist bicuculline (BIC, 10 μM). The average response to 3 μM GABA was summarized in Fig. 5A (lower panel), where the data for each cell have been normalized to cell capacitance (an index of cell size) and expressed as current density (I_{GABA}, pA/pF). Average I_{GABA} from estrus and diestrus DGGCs were significantly different. Previous studies in human embryonic kidney 293T cells with specific recombinant $GABA_A$Rs expressed have shown that the cells with expression of γ2-subunit containing receptors produce larger currents as compared to cells with expression of δ-subunit containing receptors (Bianchi and Macdonald, 2003). Consistent with this finding, I_{GABA} in CA1PCs were 2-fold higher than in DGGCs (Fig. 5A, n= 12-20).

We next assessed the ability of AP to potentiate currents on $GABA_A$Rs gated by 3 μM GABA. In acutely dissociated CA1PCs and DGGCs from estrus or diestrus stages, neurons were pre-applied with AP for 5 seconds and then GABA was co-applied with AP for 5 seconds. AP is an allosteric modulator of $GABA_A$Rs and produces little direct effect at nanomolar concentrations (Reddy, 2009). AP caused a concentration-dependent increase (I_{NS}) in peak-current responses evoked by GABA (Fig. 5C). At 10 nM AP, the mean fractional potentiation (ratio of AP+GABA to GABA alone; presented as I_{NS}/I_{GABA}) were 1.47- and 1.15-fold in DGGCs from diestrus or estrus stages, respectively (n=9-10, $p>0.05$). At 1 μM AP, the peak amplitudes obtained were 7.14- and 4.25-fold greater in DGGCs from diestrus or estrus stages, and were 4.51- and 3.01-fold greater in CA1PCs from diestrus or estrus stages, respectively (Fig. 5D, n=5-8, $p<0.05$). The data could not be Hill curve fit because no response plateau was achieved even at high concentrations. However, it is highly unlikely that the AP responses illustrated in Fig.5CD are due to direct activation of $GABA_A$Rs because direct activation occurs at concentrations higher than 1 μM used in this study. We directly tested this possibility with 1 μM AP in both DGGCs and CA1 cells without GABA (not shown). The baseline changed observed were less than 5% if compared with 1 μM AP + 3 μM GABA's response. Moreover, traces in Fig.5C, at 1 μM AP perfused for 5 sec prior to GABA, indicate lack of significant chloride current. In addition, the potentiating effects of AP in female mice were comparable with the testosterone-derived neurosteroid androstanediol in male mice (Reddy and Jian, 2010) with exception of higher potentiation in DGGCs of diestrus stage. The latter might be related to higher δ-subunit in DGGCs of diestrus versus DGGCs of male mice. Thus, these results are consistent with greater sensitivity of δ-subunit containing $GABA_A$ receptors to neurosteroids.

JPET Fast Forward. Published on May 10, 2013 as DOI: 10.1124/jpet.113.203653
This article has not been copyedited and formatted. The final version may differ from this version.

Cyclical Alterations in Neurosteroid-Sensitive Extrasynaptic $GABA_A$ Receptor-Mediated Tonic Currents During the Estrous Cycle. To further investigate the effect of elevated levels of δ-subunit expression on the functional changes in perisynaptic or extrasynaptic GABAergic inhibition, we recorded the GABA-gated tonic currents in CA1PCs and DGGCs in hippocampal slice preparations, in which most synapses and dendrites remain intact. CA1PCs and DGGCs are distinct neuronal populations in which tonic inhibition is mediated by α5-, γ-containing $GABA_A$Rs in CA1PCs where δ-subunits are scarce, and by δ-containing receptors in DGGCs (Stell et al., 2003; Caraiscos et al., 2004; Maguire et al., 2005). For analysis of tonic currents, mean peak tonic conductance (G_{tonic}) and holding root-mean-square noise conductance (G_{rms}) were measured (Fig. 6). The control G_{tonic} was measured as the difference between initial current before GABA application and current in the presence of BIC. Control G_{tonic} in DGGCs in diestrus was 3–fold larger compared to estrus at holding potential of −60 mV (Fig. 6A and 6E; n=9 -11 cells, $p<0.05$). However, there was no significant difference in the tonic conductance recorded in CA1PCs in diestrus compared to estrus. Perfusion of 3 μM GABA was used to model extracellular GABA concentration in vivo (Timmerman and Westerink, 1997; Shin et al., 2002; Rajasekaran et al., 2010) which is believed to selectively activate $GABA_A$R-mediated tonic inhibition without largely altering synaptic currents. 3 μM GABA significantly increased tonic current (Fig. 6A). The G_{tonic} in DGGCs of diestrus after application of GABA was significantly greater as compared to CA1PCs of diestrus as well as CA1PCs and DGGCs in estrus (Fig. 6E, n=5-12,). The lack of G_{tonic} changes in the CA1 region between estrus and diestrus, in which $GABA_A$R δ-subunit expression was low, is consistent with the hypothesis that selective regulation in tonic current is mediated by δ-subunits during the ovarian cycle (Pirker et al., 2000; Wei et al., 2003; Maguire et al., 2005). In addition, during application of 3 μM GABA, the inward tonic current reached the peak (G_{tonic}) and then decayed to persistent, low desensitized current, which did not return to the baseline in the given time. The desensitization/decay of DGGCs of diestrus was 8% from the peak of G_{tonic} and was significantly smaller than decrease of 17% in estrus stage DGGCs, 27% decrease in diestrus CA1PCs, and 45% decrease in estrus CA1PCs.

The G_{rms}, represented as noise conductance from chloride ions passing through the opened channels before and after application of GABA with BIC, was examined (Fig.6). In response to BIC, a slow outward current occurred as mentioned above, accompanied by reduction in baseline noise. The G_{rms} in DGGCs of diestrus was 9.22 ± 0.98 pS/pF during baseline period, 19.28 ± 1.16 pS/pF at 3 minutes following application of 3 μM GABA, and 8.27 ± 0.93 pS/pF at 2 minutes after application of GABA + 10 μM BIC (Fig. 6B and 6F). The distribution of G_{rms} measurements after application of GABA in DGGCs of diestrus was significantly increased as determined by the Kolmogorov-Smirnov test (Fig. 6C). To further understand the impact of 3 μM GABA on G_{rms}, a G_{rms} amplitude-events

JPET Fast Forward. Published on May 10, 2013 as DOI: 10.1124/jpet.113.203653
This article has not been copyedited and formatted. The final version may differ from this version.

distribution histogram was created, which demonstrates that GABA increased the frequency of large G_{rms} (Fig. 6D). The summarized data of G_{rms} in DGGCs of diestrus after application of GABA was significantly greater as compared to DGGCs of estrus, and CA1PCs of diestrus and estrus (Fig. 6F, n=5-12). These results further confirm that ovarian cycle-related, $GABA_A$ receptor δ-subunit regulation contributes to tonic inhibitory current.

The neurosteroid AP significantly enhanced $GABA_AR$-mediated currents in DGGCs (Fig.6GH). AP is likely to be found slightly higher in the hippocampus in vivo and δ-$GABA_ARs$ are highly sensitive to AP (Maguire et al., 2005; Mtchedlishvili and Kapur, 2006; Maguire and Mody, 2007). We investigated the modulation of extrasynaptic tonic current by 300 nM AP in the presence of 3 μM GABA. The G_{tonic} and G_{rms} were enhanced by 300 nM AP in DGGCs of diestrus (Fig. 6G). Compared to GABA alone, AP enhanced G_{tonic} by 2.6-fold and G_{rms} by 1.2-fold in DGGCs of diestrus ($p<0.05$). However, there were no significant differences on tonic inhibition between GABA alone and GABA + AP groups in CA1PCs (Fig. 6H). We used 300 nM AP to uncover the δ-subunit specific effects of neurosteroids on tonic conductance because δ-containing $GABA_ARs$ display greater sensitivity to neurosteroids at physiological or supraphysiological levels. Although the exact physiological levels of AP in the extracellular space within the hippocampus are unknown, the levels may range from 10 nM to 120 nM, depending on the physiological or other conditions such as estrous cycle or pregnancy (Murri L and Galli, 1997; Bernardi et al., 1998; Concas et al., 1998; Genazzani et al., 1998; Tuveri et al., 2008; Reddy, 2009). Even at low or physiological levels (30 nM), AP can elicit similar greater response in diestrus than estrus stage per the standard linear concentration-response relationship (fractional response of maximal peak current). These results clearly suggest that tonic inhibition is modulated by $GABA_AR$ δ-subunit plasticity and can be significantly potentiated by the neurosteroid AP during the diestrus stage.

Alterations in Susceptibility to Limbic Epileptogenesis During the Estrous Cycle. To investigate whether the cycle-related plasticity of $GABA_ARs$ mediating phasic and tonic inhibition affect neuronal network excitability in a seizure model, we studied the susceptibility of mice to epileptogenesis in rapid hippocampus kindling (Reddy and Mohan, 2011; Reddy et al., 2012). The progression of rate of kindling, electrographic mean afterdischarge (AD) threshold, and cumulative AD activity time for kindling criterion were recorded as main indices of epileptogenesis (Fig. 7). Mice in diestrus stage showed a significant resistance to the development of kindling epileptogenesis, as evident in the increased number of stimulations required to elicit behavioral seizures compared with estrus mice. The rate of kindling, expressed as the number of stimulations required to induce stage 4/5 seizures, was significantly slower in diestrus mice compared with estrus mice (Fig. 7A). No

significant differences in the current required to trigger the initial AD were evident between estrus and diestrus groups (Fig. 7B). In addition, there was no difference in the total electrographic activity between estrus and diestrus groups (Fig.7C). Representative AD traces are illustrated in Fig. 7D. We found that mice at estrus showed high amplitude electrographic discharges during kindling development as compared to diestrus stage (Fig.7D). To ascertain the influence of drug-induced elevations in tonic currents on epileptogenesis, we examined the effect of AP on kindling epileptogenesis progression at estrus and diestrus stages. During kindling sessions, animals were injected with AP (3 mg/kg, s.c.) 15 minutes before stimulations. AP-treated mice at diestrus stage showed significant suppression of behavioral seizure activity compared with estrus group (Fig.7A). Similarly, AP-treated mice at diestrus required protracted electrographic seizure activity for reaching the kindling criterion as compared to mice at estrus stage (Fig. 7C). The amplitude of AD spike activity was markedly reduced in AP-treated mice at diestrus stage (Fig.7D). Thus, these results are consistent with the increased expression of δ-subunit during diestrus stage, which confers greater sensitivity to neurosteroid suppression of seizures and epileptogenesis.

JPET Fast Forward. Published on May 10, 2013 as DOI: 10.1124/jpet.113.203653
This article has not been copyedited and formatted. The final version may differ from this version.

Discussion

The ovarian cycle is generally recognized as a key regulator $GABA_AR$s plasticity and function. The present study shows that cyclical elevation in progesterone levels in diestrus are accompanied with subfield-specific increased extrasynaptic $GABA_AR$ δ-subunit expression in the hippocampus. Increase in tonic inhibition and decrease in seizure susceptibility are functional consequences of this plasticity. Allopregnanolone strongly potentiated tonic inhibition and has powerful protective activity in the hippocampus kindling model of epileptogenesis during diestrus stage. Collectively, these novel findings provide molecular and cellular basis of neurosteroid dynamics in estrous cycle-regulated neuronal excitability and seizure susceptibility, strongly implicated to play an important role in menstrual cycle-related brain conditions such as catamenial epilepsy, premenstrual syndrome and migraine.

The precise subunit plasticity in the hippocampus during the estrous cycle is not clearly understood. However, there is evidence that cyclical fluctuations in steroid hormones across the estrous cycle regulate several $GABA_AR$ subunits (Maguire et al., 2005; Gangisetty and Reddy, 2010; Reddy et al., 2012). Previous studies reported that compared to estrus, diestrus δ-subunit is increased, γ2-subunit is decreased, and α4-subunit exhibits no change (Maguire et al., 2005). Another study demonstrated δ-subunit response to progesterone treatment in an isolated culture system (Mostallino et al., 2006). The current study utilizes endogenous fluctuations in progesterone and neurosteroids across the estrous cycle to examine expressional and functional subunit plasticity in the hippocampal subfields. We used highly sensitive, optimized assays for subunit mRNA expression and subsequent western blot analysis (Gangisetty and Reddy, 2009). Furthermore, we focused on individual hippocampus subfields, in which we report regulation of $GABA_AR$ expression to be subfield-specific. We found greater α1 expression in CA1 and DG and higher α2 and δ expression in CA3 and DG during diestrus compared to estrus. Moreover, there was no change in α4 and γ2 expression in diestrus (Fig.2). Our data on δ and α4 expression are consistent with previous studies (Maguire et al., 2005; Maguire and Mody, 2007). In contrast to previous reports, we observed no significant change in subfield γ2 expression. Differences could be due to previous studies' protein analysis in the whole hippocampus as measure of change, whereas we investigated mRNA in individual subfields, allowing greater signal sensitivity. The α4- and δ-subunits preferentially co-assemble in DGGC extrasynaptic membranes (Mostallino et al., 2006; Maguire and Mody, 2009). Since diestrus results in increase of δ but not α4, other α-subunits may increase to co-assemble with δ subunit.

JPET Fast Forward. Published on May 10, 2013 as DOI: 10.1124/jpet.113.203653
This article has not been copyedited and formatted. The final version may differ from this version.

In the present study, diestrus subunit increases of α1 and α2 in DG, α1 within CA1, and α2 within CA3 are novel observations of primarily synaptic α-subunit plasticity in estrous cycle. α1βδ receptors possess low desensitization kinetics and neurosteroid sensitivity similar to α4βδ (Bianchi and Macdonald, 2002; Zheleznova et al., 2008). The α1 could plausibly assemble with δ extrasynaptically. Emerging evidence suggests that α2 is involved in synaptic targeting; moreover, α2β3δ receptors have very low GABA potency (Wu et al., 2012). Therefore, it is unlikely that α2-containing receptors assemble extrasynaptically with δ-subunit or respond to low micromolar extracellular GABA to gate tonic inhibition. Nevertheless, substantial increases in synaptic α2 could affect overall neuronal excitability. The α2βγ2 receptor has faster activation kinetics, prolonged open duration and bursting activity, and slower deactivation/decay time than α1βγ2 (Lavoie et al., 1997). A large switch from α1- to α2-containing receptors in the hypothalamus has been previously shown to be coupled with slower postsynaptic current decay (Brussaard et al., 1997; Brussaard and Herbison, 2000). Therefore, an increased α2-subunit proportion could result in greater net inhibitory postsynaptic current. More investigation is required to understand if cycle-related α-subunit plasticity within the hippocampus modulates synaptic activity.

We observed that diestrus δ-subunit increase within DG has positive modulatory effects on tonic inhibition. Furthermore, increase in AP potentiation of whole-cell and tonic currents during diestrus is mainly δ-directed. The δ-subunit has potent transduction properties to increase opening of $GABA_AR$ channels in the presence of AP (Brown et al., 2002). There is subtle effect of the estrous cycle-related δ-subunit plasticity on GABA sensitivity in DGGCs with a marginal 12% greater sensitivity at diestrus stage (Fig.5). Our observations of increased δ-subunit expression (Fig.2,3) in diestrus DGGCs may contribute to increased GABAergic currents (Fig.5), tonic inhibition, persistent opening of $GABA_AR$ channels (Fig.6), and reductions in seizure susceptibility (Fig.7). There were little alterations of tonic inhibition or AP sensitivity in CA1PCs at diestrus and estrus stages. Therefore, the enhanced neurosteroid sensitivity and reduced seizure susceptibility at diestrus are ascribed to the relative increase in δ-subunit in the dentate gyrus. Further, these responses may be due to either greater tonic current or higher levels of endogenous AP at diestrus stage. However, it is unlikely that differences in ambient GABA level at diestrus are the main factor for such greater tonic current responses. First, the increase in δ-subunit is associated with greater current to both GABA and AP. We found this response in DGGCs but not in CA1 cells (Fig. 6E). Second, application of BIC blocked the tonic currents and the resulting fractional blockade was equivalent to that of control (ambient GABA) values, indicating subtle differences in endogenous GABA.

JPET Fast Forward. Published on May 10, 2013 as DOI: 10.1124/jpet.113.203653
This article has not been copyedited and formatted. The final version may differ from this version.

Aging is associated with low levels of progesterone/neurosteroid in the brain and may profoundly affect anxiety and seizure susceptibility (Reddy, 2003; Reddy, 2009; Reddy and Jian, 2010). $GABA_AR$ δ-subunit expression in ovariectomized and aged, acyclic mice showed no differences to that of diestrus (Fig.4A), indicating that the estrous cycle-related changes in subunit plasticity is due to the cyclical changes instead of the relative levels of different hormones. The observation that δ-subunit levels are high in aged and ovariectomized animals despite lower progesterone levels provides strong credence to the premise that, in intact cycling females, the distinct hormonal milieu at estrus stage may be restraining δ-subunit expression followed by disinhibition at diestrus stage. Therefore, undiminished δ-subunit expression in ovariectomized and acyclic aged mice might be related to compensatory mechanism or local neurosteroid synthesis.

Our results suggest that PRs are not responsible for the estrous cycle regulation of δ-subunit expression. Previously we showed that progesterone's anti-seizure effects are preserved (Reddy et al., 2004) and development of epileptogenesis is delayed in PRKO mice (Reddy and Mohan, 2011). Progesterone-related upregulation of δ from estrus to diestrus was retained in PRKO mice (Fig.4B). Increase in δ-subunit in both WT and PRKO was inhibited by finasteride block of AP synthesis. These results are consistent with the previous report on the role of PR (Maguire and Mody, 2007). Similar subunit plasticity, observed in $GABA_AR$ expression upon neurosteroid withdrawal, is independent of the PR pathway (Gangisetty and Reddy, 2010). We conclude that PRs does not play a role in regulation of δ-subunit expression and this plasticity is neurosteroid-dependent.

A key observation of this study is that finasteride can prevent the increase in δ-subunits on diestrus, suggesting that endogenous neurosteroids, such as AP, on diestrus may be the trigger for δ-subunit expression. However, the molecular mechanism of neurosteroid upregulation of δ-subunit expression remains unclear. A variety of mechanisms could contribute to the neurosteroid-mediated estrous cycle regulation of $GABA_ARs$ plasticity (Kuver et al, 2012; Abramian et al., 2010; Joshi and Kapur, 2009). The neurosteroid AP is synthesized *de novo* within neurons (Reddy, 2009; 2013), and circulating AP levels parallel those of precursor progesterone (Tuveri et al., 2008). Although the dynamics of brain AP during the menstrual cycle are not well studied, it is likely local synthesis of neurosteroids occurs in key regions of the limbic system including hippocampus and amygdala (Agis-Balboa et al., 2006; Ebner et al., 2006; Mukai et al., 2008). $GABA_AR$ heterogeneity confers different neurosteroid binding affinities and gating. $\alpha1\beta2\gamma2$ and $\alpha2\beta2\gamma2$ $GABA_ARs$ are abundant in the hippocampus and have relatively low neurosteroid sensitivity. $\alpha1\beta\delta$ and $\alpha4\beta\delta$ compositions are

present in DG and have high neurosteroid sensitivity/affinity. AP potentiation of I_{GABA} from diestrus DGGCs was significantly larger than from diestrus CA1PCs, and estrus CA1PCs and DGGCs (Fig.5,6). These changes contribute to reduced seizure susceptibility such as that occurs during the luteal phase in women with catamenial epilepsy.

Figure 8 depicts the proposed effects of the estrous cycle on $GABA_AR$ plasticity and function. During estrus, progesterone is low; transcriptional regulation is shifted away from δ-subunit expression. During diestrus, progesterone is substantially increased systemically and within the brain. This results in appreciable increase in neurosteroid synthesis. Abundance of neurosteroid couples an increase in δ-subunit expression within the neuron, conferring greater production of δ-containing $GABA_ARs$ at extrasynaptic sites within the membrane. These receptors are distinctively more sensitive to neurosteroid binding, and tonic inhibition is enhanced. Allopregnanolone produces greater positive modulation of tonic inhibition and thereby reduces seizure susceptibility during the diestrus. These observations are clinically relevant in women with epilepsy and other hormone-sensitive brain conditions such as premenstrual syndrome and migraine.

In perimenstrual catamenial epilepsy, evidence suggests that progesterone level changes play a key role in seizure exacerbations (Reddy, 2009; 2012). Greater seizure activity within estrus stage is demonstrated in the hippocampus kindling model of epileptogenesis (Fig.7). Heightened seizure susceptibility is consistent with previous reports in related models of neurosteroid withdrawal, pseudopregnancy, and ovarian cycle (Smith et al., 1998a; 1998b; Reddy et al., 2001; Gangisetty and Reddy, 2010). The basis for enhanced seizure susceptibility in perimenstrual catamenial epilepsy may be due to the withdrawal of neurosteroids around the time of menstruation (Reddy et al., 2001; 2012). Although some studies show progesterone and its metabolites regulate $GABA_ARs$ to affect seizure susceptibility, they are limited to exogenous application of progesterone or studying few subunits (Smith et al., 1998ab; Maguire et al., 2005). Our present study shows overt changes in seizure susceptibility over the estrous cycle and in response to AP. Seizure susceptibility was decreased during diestrus due to enhanced $GABA_AR$ tonic inhibition in which progesterone/AP levels were elevated and δ-subunit expression was increased. Specific δ-subunit regulation within the ovarian cycle is important to define molecular mechanisms for catamenial epilepsy. Thus, δ-containing $GABA_ARs$ may be a potential therapeutic target in epilepsy treatment. Neurosteroid agents that augment tonic inhibition and lack benzodiazepine-like side effects have shown promise in treatment of epilepsy in women (Reddy, 2010; Pack et al., 2011).

In conclusion, this study demonstrates estrous cycle-related, neurosteroid-dependent cyclical alterations in extrasynaptic δ-subunit-containing $GABA_AR$ plasticity and function in the hippocampus. Neurosteroid regulation of δ-containing $GABA_ARs$ may represent rational molecular mechanisms for menstrual cycle-induced alterations in neuronal excitability and seizure susceptibility, especially in catamenial epilepsy and related menstrual conditions linked to deficiencies in tonic inhibition. These mechanisms are also relevant to premenstrual syndrome, migraine and other menstrual cycle-related brain conditions in women.

Acknowledgements

The authors acknowledge the support of the Texas A&M Health Science Center Women's Health in Neuroscience (WHIN) program. We thank Drs. William Griffith, David Murchison, Gerald Frye and Dustin DuBois for help with tonic current recordings in hippocampal slices.

Author contributions

Participated in research design: Reddy.

Conducted experiments: Reddy, Gangisetty, Wu and Carver.

Performed data analysis: Reddy, Gangisetty, Wu and Carver.

Contributed new reagents or analytic tools: Reddy

Wrote or contributed to the writing of the manuscript: Reddy, Wu and Carver

References

Abramian AM, Comenencia-Ortiz E, Vithlani M, Tretter EV, Sieghart W, Davies PA and Moss SJ (2010) Protein kinase C phosphorylation regulates membrane insertion of $GABA_A$ receptor subtypes that mediate tonic inhibition. *J Biol Chem* **285**:41795-41805.

Agis-Balboa RC, Pinna G, Zhubi A, Maloku E, Veldic M, Costa E and Guidotti A (2006) Characterization of brain neurons that express enzymes mediating neurosteroid biosynthesis. *Proc Natl Acad Sci USA* **103**:14602-14607.

Backstrom T, Andersson A, Andree L, Birzniece V, Bixo M, Bjorn I, Haage D, Isaksson M, Johansson IM, Lindblad C, Lundgren P, Nyberg S, Odmark IS, Stromberg J, Sundstrom-Poromaa I, Turkmen S, Wahlstrom G, Wang M, Wihlback AC, Zhu D and Zingmark E (2003) Pathogenesis in menstrual cycle-linked CNS disorders. *Ann N Y Acad Sci* **1007**:42-53.

Belelli D, Casula A, Ling A and Lambert JJ (2002) The influence of subunit composition on the interaction of neurosteroids with $GABA_A$ receptors. *Neuropharmacology* **43**:651-661.

Bernardi F, Hartmann B, Casarosa E, Luisi S, Stomati M, Fadalti M, Florio P, Santuz M, Luisi M, Petraglia F and Genazzani AR (1998a) High levels of serum allopregnanolone in women with premature ovarian failure. *Gynecol Endocrinol* **12**:339-345.

Bernardi F, Salvestroni C, Casarosa E, Nappi RE, Lanzone A, Luisi S, Purdy RH, Petraglia F and Genazzani AR (1998b) Aging is associated with changes in allopregnanolone concentrations in brain, endocrine glands and serum in male rats. *Eur J Endocrinol* **138**:316-321.

Bianchi MT and Macdonald RL (2003) Neurosteroids shift partial agonist activation of $GABA_A$ receptor channels from low- to high-efficacy gating patterns. *J Neurosci* **23**:10934-10943.

Brown N, Kerby J, Bonnert TP, Whiting PJ and Wafford KA (2002) Pharmacological characterization of a novel cell line expressing human $\alpha4\beta3\delta$ $GABA_A$ receptors. *Br J Pharmacol* **136**:965-974.

Brussaard AB and Herbison AE (2000) Long-term plasticity of postsynaptic GABAA-receptor function in the adult brain: insights from the oxytocin neurone. *Trends Neurosci* **23**:190-195.

Brussaard AB, Kits KS, Baker RE, Willems WP, Leyting-Vermeulen JW, Voorn P, Smit AB, Bicknell RJ and Herbison AE (1997) Plasticity in fast synaptic inhibition of adult oxytocin neurons caused by switch in $GABA_A$ receptor subunit expression. *Neuron* **19**:1103-1114.

Caraiscos VB, Elliott EM, You-Ten KE, Cheng VY, Belelli D, Newell JG, Jackson MF, Lambert JJ, Rosahl TW, Wafford KA, MacDonald JF and Orser BA (2004) Tonic inhibition in mouse hippocampal CA1 pyramidal neurons is mediated by $\alpha5$ subunit-containing gamma-aminobutyric acid type A receptors. *Proc Natl Acad Sci USA* **101**:3662-3667.

Chappell PE, Lydon JP, Conneely OM, O'Malley BW and Levine JE (1997) Endocrine defects in mice carrying a null mutation for the progesterone receptor gene. *Endocrinology* **138**:4147-4152.

Concas A, Mostallino MC, Porcu P, Follesa P, Barbaccia ML, Trabucchi M, Purdy RH, Grisenti P and Biggio G (1998) Role of brain allopregnanolone in the plasticity of gamma-aminobutyric acid type A receptor in rat brain during pregnancy and after delivery. *Proc Natl Acad Sci USA* **95**:13284-13289.

Ebner MJ, Corol DI, Havlikova H, Honour JW and Fry JP (2006) Identification of neuroactive steroids and their precursors and metabolites in adult male rat brain. *Endocrinology* **147**:179-190.

Gangisetty O and Reddy DS (2009) The optimization of TaqMan real-time RT-PCR assay for transcriptional profiling of $GABA_A$ receptor subunit plasticity. *J Neurosci Methods* **181**:58-66.

Gangisetty O and Reddy DS (2010) Neurosteroid withdrawal regulates $GABA_A$ receptor α4-subunit expression and seizure susceptibility by activation of progesterone receptor-independent early growth response factor-3 pathway. *Neuroscience* **170**:865-880.

Genazzani AR, Petraglia F, Bernardi F, Casarosa E, Salvestroni C, Tonetti A, Nappi RE, Luisi S, Palumbo M, Purdy RH and Luisi M (1998) Circulating levels of allopregnanolone in humans: gender, age, and endocrine influences. *J Clin Endocrinol Metab* **83**:2099-2103.

Herzog AG, Fowler KM, Sperling MR, Liporace JD, Kalayjian LA, Heck CN, Krauss GL, Dworetzky BA and Pennell PB (2011) Variation of seizure frequency with ovulatory status of menstrual cycles. *Epilepsia* **52**:1843-1848.

Herzog AG and Frye CA (2003) Seizure exacerbation associated with inhibition of progesterone metabolism. *Ann Neurol* **53**:390-391.

Herzog AG, Harden CL, Liporace J, Pennell P, Schomer DL, Sperling M, Fowler K, Nikolov B, Shuman S and Newman M (2004) Frequency of catamenial seizure exacerbation in women with localization-related epilepsy. *Annals of neurology* **56**:431-434.

Hosie AM, Wilkins ME and Smart TG (2007) Neurosteroid binding sites on $GABA_A$ receptors. *Pharmacol Ther* **116**:7-19.

Joshi S and Kapur J (2009) Slow intracellular accumulation of $GABA_A$ receptor delta subunit is modulated by brain-derived neurotrophic factor. *Neuroscience* **164**:507-519.

Kay AR and Wong RK (1986) Isolation of neurons suitable for patch-clamping from adult mammalian central nervous systems. *J Neurosci Methods* **16**:227-238.

Kuver A, Shen H and Smith SS (2012) Regulation of the surface expression of alpha4beta2delta $GABA_A$ receptors by high efficacy states. *Brain Res* **1463**:1-20.

Lavoie AM, Tingey JJ, Harrison NL, Pritchett DB and Twyman RE (1997) Activation and deactivation rates of recombinant $GABA_A$ receptor channels are dependent on α-subunit isoform. *Biophys J* **73**:2518-2526.

Lothman EW and Williamson JM (1993) Rapid kindling with recurrent hippocampal seizures. *Epilepsy Res* **14**:209-220.

Lu KH, Hopper BR, Vargo TM and Yen SS (1979) Chronological changes in sex steroid, gonadotropin and prolactin secretions in aging female rats displaying different reproductive states. *Biol Reprod* **21**:193-203.

Lydon JP, DeMayo FJ, Funk CR, Mani SK, Hughes AR, Montgomery CA, Jr., Shyamala G, Conneely OM and O'Malley BW (1995) Mice lacking progesterone receptor exhibit pleiotropic reproductive abnormalities. *Genes Dev* **9**:2266-2278.

Maguire J, Ferando I, Simonsen C and Mody I (2009) Excitability changes related to $GABA_A$ receptor plasticity during pregnancy. *J Neurosci* **29**:9592-9601.

Maguire J and Mody I (2007) Neurosteroid synthesis-mediated regulation of $GABA_A$ receptors: relevance to the ovarian cycle and stress. *J Neurosci* **27**:2155-2162.

Maguire J and Mody I (2009) Steroid hormone fluctuations and $GABA_A$R plasticity. *Psychoneuroendocrinology* **34(Suppl 1)**:S84-90.

Maguire JL, Stell BM, Rafizadeh M and Mody I (2005) Ovarian cycle-linked changes in $GABA_A$ receptors mediating tonic inhibition alter seizure susceptibility and anxiety. *Nat Neurosci* **8**:797-804.

Mangan PS, Sun C, Carpenter M, Goodkin HP, Sieghart W and Kapur J (2005) Cultured hippocampal pyramidal neurons express two kinds of $GABA_A$ receptors. *Mol Pharmacol* **67**:775-788.

Molina-Hernandez M, Contreras CM and Tellez-Alcantara P (2001) Diazepam increases the number of punished responses in a conflict-operant paradigm during late proestrus and estrus in the Wistar rat. *Neuropsychobiology* **43**:29-33.

Mostallino MC, Mura ML, Maciocco E, Murru L, Sanna E and Biggio G (2006) Changes in expression of the delta subunit of the $GABA_A$ receptor and in receptor function induced by progesterone exposure and withdrawal. *J Neurochem* **99**:321-332.

Mtchedlishvili Z and Kapur J (2006) High-affinity, slowly desensitizing $GABA_A$ receptors mediate tonic inhibition in hippocampal dentate granule cells. *Mol Pharmacol* **69**:564-575.

Mukai Y, Higashi T, Nagura Y and Shimada K (2008) Studies on neurosteroids XXV. Influence of a 5α-reductase inhibitor, finasteride, on rat brain neurosteroid levels and metabolism. *Biol Pharm Bull* **31**:1646-1650.

Murri L and Galli R (1997) Catamenial epilepsy, progesterone and its metabolites. *Cephalalgia* **17 Suppl 20**:46-47.

Pack AM, Reddy DS, Duncan S and Herzog A (2011) Neuroendocrinological aspects of epilepsy: Important issues and trends in future research. *Epilepsy Behav* **22**:94-102.

Pirker S, Schwarzer C, Wieselthaler A, Sieghart W and Sperk G (2000) $GABA_A$ receptors: immunocytochemical distribution of 13 subunits in the adult rat brain. *Neuroscience* **101**:815-850.

Racine RJ (1972) Modification of seizure activity by electrical stimulation. II. Motor seizure. *Electroencephalogr Clin Neurophysiol* **32**:281-294.

Rajasekaran K, Joshi S, Sun C, Mtchedlishvilli Z and Kapur J (2010) Receptors with low affinity for neurosteroids and GABA contribute to tonic inhibition of granule cells in epileptic animals. *Neurobiol Dis* **40**:490-501.

Reddy DS (2003) Pharmacology of endogenous neuroactive steroids. *Crit Rev Neurobiol* **15**:197-234.

Reddy DS (2004) Anticonvulsant activity of the testosterone-derived neurosteroid 3α-androstanediol. *Neuroreport* **15**:515-518.

Reddy DS (2009) The role of neurosteroids in the pathophysiology and treatment of catamenial epilepsy. *Epilepsy Res* **85**:1-30.

Reddy DS (2010) Neurosteroids: endogenous role in the human brain and therapeutic potentials. *Prog Brain Res* **186**:113-137.

Reddy DS (2013) Neuroendocrine aspects of catamenial epilepsy. *Horm Behav* **63**:254-266.

Reddy DS, Castaneda DC, O'Malley BW and Rogawski MA (2004) Anticonvulsant activity of progesterone and neurosteroids in progesterone receptor knockout mice. *J Pharmacol Exp Ther* **310**:230-239.

Reddy DS, Gould J and Gangisetty O (2012) A mouse kindling model of perimenstrual catamenial epilepsy. *J Pharmacol Exp Ther* **341**:784-793.

Reddy DS and Jian K (2010) The testosterone-derived neurosteroid androstanediol is a positive allosteric modulator of $GABA_A$ receptors. *J Pharmacol Exp Ther* **334**:1031-1041.

Reddy DS, Kim HY and Rogawski MA (2001) Neurosteroid withdrawal model of perimenstrual catamenial epilepsy. *Epilepsia* **42**:328-336.

Reddy DS and Kulkarni SK (1999) Sex and estrous cycle-dependent changes in neurosteroid and benzodiazepine effects on food consumption and plus-maze learning behaviors in rats. *Pharmacol Biochem Behav* **62**:53-60.

Reddy DS and Mohan A (2011) Development and persistence of limbic epileptogenesis are impaired in mice lacking progesterone receptors. *J Neurosci* **31**:650-658.

Reddy DS, O'Malley BW and Rogawski MA (2005) Anxiolytic activity of progesterone in progesterone receptor knockout mice. *Neuropharmacology* **48**:14-24.

Shen H, Gong QH, Aoki C, Yuan M, Ruderman Y, Dattilo M, Williams K and Smith SS (2007) Reversal of neurosteroid effects at alpha4beta2delta $GABA_A$ receptors triggers anxiety at puberty. *Nat Neurosci* **10**:469-477.

Shen H, Sabaliauskas N, Sherpa A, Fenton AA, Stelzer A, Aoki C and Smith SS (2010) A critical role for$\alpha4\beta\delta$ $GABA_A$ receptors in shaping learning deficits at puberty in mice. *Science* **327**:1515-1518.

Shin RS, Anisman H, Merali Z and McIntyre DC (2002) Changes in extracellular levels of amygdala amino acids in genetically fast and slow kindling rat strains. *Brain Res* **946**:31-42.

Smith SS, Gong QH, Hsu FC, Markowitz RS, ffrench-Mullen JM and Li X (1998a) $GABA_A$ receptor $\alpha4$ subunit suppression prevents withdrawal properties of an endogenous steroid. *Nature* **392**:926-930.

Smith SS, Gong QH, Li X, Moran MH, Bitran D, Frye CA and Hsu FC (1998b) Withdrawal from 3alpha-OH-5alpha-pregnan-20-One using a pseudopregnancy model alters the kinetics of hippocampal GABAA-gated current and increases the $GABA_A$ receptor $\alpha4$ subunit in association with increased anxiety. *J Neurosci* **18**:5275-5284.

Steger RW and Peluso JJ (1982) Effects of age on hormone levels and in vitro steroidogenesis by rat ovary and adrenal. *Exp Aging Res* **8**:203-208.

Stell BM, Brickley SG, Tang CY, Farrant M and Mody I (2003) Neuroactive steroids reduce neuronal excitability by selectively enhancing tonic inhibition mediated by δ subunit-containing $GABA_A$ receptors. *Proc Natl Acad Sci USA* **100**:14439-14444.

Tangney JR, Chuang JS, Janssen MS, Krishnamurthy A, Liao P, Hoshijima M, Wu X, Meininger GA, Muthuchamy M, Zemljic-Harpf A, Ross RS, Frank LR, McCulloch AD and Omens JH (2013) Novel role for vinculin in ventricular myocyte mechanics and dysfunction. *Biophys J* **104**:1623-1633.

Timmerman W and Westerink BH (1997) Brain microdialysis of GABA and glutamate: what does it signify? *Synapse* **27**:242-261.

Tuveri A, Paoletti AM, Orru M, Melis GB, Marotto MF, Zedda P, Marrosu F, Sogliano C, Marra C, Biggio G and Concas A (2008) Reduced serum level of THDOC, an anticonvulsant steroid, in women with perimenstrual catamenial epilepsy. *Epilepsia* **49**:1221-1229.

Uusi-Oukari M and Korpi ER (2010) Regulation of $GABA_A$ receptor subunit expression by pharmacological agents. *Pharmacol Rev* **62**:97-135.

van Broekhoven F and Verkes RJ (2003) Neurosteroids in depression: a review. *Psychopharmacology (Berl)* **165**:97-110.

Wei W, Zhang N, Peng Z, Houser CR and Mody I (2003) Perisynaptic localization of delta subunit-containing $GABA_A$ receptors and their activation by GABA spillover in the mouse dentate gyrus. *J Neurosci* **23**:10650-10661.

Wu X, Sun Z, Foskett A, Trzeciakowski JP, Meininger GA and Muthuchamy M (2010) Cardiomyocyte contractile status is associated with differences in fibronectin and integrin interactions. *Am J Physiol Heart Circ Physiol* **298**:H2071-2081.

Wu X, Wu Z, Ning G, Guo Y, Ali R, Macdonald RL, De Blas AL, Luscher B and Chen G (2012) Gamma-aminobutyric acid type A ($GABA_A$) receptor α subunits play a direct role in synaptic versus extrasynaptic targeting. *J Biol Chem* **287**:27417-27430.

Zheleznova N, Sedelnikova A and Weiss DS (2008) $\alpha1\beta2\delta$, a silent $GABA_A$ receptor: recruitment by tracazolate and neurosteroids. *Br J Pharmacol* **153**:1062-1071.

Footnote to title page

This research was supported by the National Institutes of Health National Institute of Neurological Disorders and Stroke [Grant NS051398].

FIGURE LEGENDS

Fig. 1. Histological features of the murine estrous cycle and progesterone levels in female mice. A, Cellular profile of eosin stained vaginal smears obtained at various stages. Diestrus is characterized by abundant leukocytes with very few parabasal cells, whereas estrus is typified by the presence of irregularly shaped, highly cornified nucleated epithelial cells. Proestrus is characterized by small irregularly shaped, non-cornified epithelial cells, whereas the hallmark of metestrus is the abundance of both epithelial cells and leukocytes. Bar = 50 µm. B, Plasma progesterone levels during estrus and diestrus. Progesterone levels were significantly higher in diestrus compared to estrus. Values represented as mean ± SEM (n=6 mice per group). *p<0.05 vs. estrus stage.

Fig. 2. Changes in $GABA_AR$ subunit expression in the hippocampus CA1, CA3, and dentate gyrus (DG) subfields over the ovarian cycle. A, B and C, TaqMan RT-PCR analysis of $GABA_AR$ subunits mRNA expression in the hippocampus. D and E, Western blot analysis of δ-subunit in the dentate gyrus at estrus and diestrus stages. D, Representative immunoblots of δ-subunit protein in estrus (E) and diestrus (DE) stages. E, Densitometric quantification of DG δ-subunit protein levels. F, mRNA copy number quantification for δ-subunit according to subfield region. The data represents the mean ± SEM (n=8 animals per group). *p<0.05 vs. estrus group.

Fig. 3. Immunocytochemical distribution of $GABA_AR$ δ-subunit in dissociated hippocampal CA1 pyramidal cells (CA1PCs) and dentate gyrus granule cells (DGGCs) over the ovarian cycle. A, Immunofluorescence labeling using anti-δ subunit primary antibody with Alexa Fluor® 555 labeled IgG (Blue). The **δ** -subunit staining intensity in DGGC was markedly greater than in cells from CA1. Bar = 10 µm. B, Normalized mean integrated densities to control IgG staining in each group before comparing between groups (n=6). C, Isolated DGGC body of diestrus labeled blue for $GABA_AR$ δ-subunit in X-Y, Y-Z and X-Z axes. The δ-subunit staining was evident at cell membrane surface (arrows). Bar=5 µm. *p<0.05 vs. DGGC in estrus. $^{\#}$p<0.05 vs. CA1 in diestrus.

Fig. 4. Effect of aging, ovariectomy and finasteride treatment on δ-subunit expression in the hippocampus subfields. A, δ-subunit mRNA expression in young (cycling), ovariectomized and aged (acyclic) mice. B, δ-subunit mRNA expression in progesterone receptor knockout (PRKO) mice. C, δ-subunit mRNA in finasteride (50 mg/kg, i.p.)-treated WT (diestrus) and PRKO mice. D, Schematic illustration of finasteride blockade of 5α-reductase enzyme involved in the biosynthesis of AP and

JPET Fast Forward. Published on May 10, 2013 as DOI: 10.1124/jpet.113.203653
This article has not been copyedited and formatted. The final version may differ from this version.

related neurosteroids. Values represent the mean ± SEM (n=8 animals per group). *p<0.05 vs. young (estrus) or WT (estrus) group; **p<0.05 vs. vehicle control group in panel C.

Fig. 5. Whole-cell GABA-gated Cl^- currents (I_{GABA}) in acutely dissociated CA1PCs and DGGCs during diestrus and estrus stages. A, Morphology of acutely dissociated hippocampal principle cells used for whole-cell recording of current, voltage-clamped at -70 mV. Bar=10 µm. Representative recordings (middle panel) from cells of CA1 and DG subfields. GABA (3 µM) activated Cl^- currents (I_{GABA}) were larger in CA1 than in DG. Lower panel: I_{GABA} peak values. Current is normalized to cell capacitance (an index of cell size) and expressed as current density (pA/pF, n = 12 to 20 cells). *p<0.05 *vs.* estrus group. B, Concentration response curves for GABA (0.1–10000 µM) evoked currents in DGGCs from estrus and diestrus. Current amplitude (I_{GABA}) values were normalized to the maximum values ($I_{GABA\text{-}MAX}$) of GABA responses in the same cells. C, Representative traces showing allopregnanolone (AP) potentiation (I_{NS}) of I_{GABA} at varying concentrations (10 nM to 1 µM) in DGGC. AP was pre-applied for 5 sec before the onset of the GABA co-application. Gray thin bars indicate application of 3 µM GABA. Solid bars indicate application of AP. D, Concentration–response curves for AP derived from experiments similar to those shown in (C). Peak amplitude values during co-application of GABA and neurosteroid were compared with the amplitude of GABA responses in the same cells (as fractional potentiation, I_{NS}/I_{GABA}). AP (n=5 to 10) produced a concentration-dependent enhancement of GABA-activated currents with no response plateau. Value bars or points represent the mean ± SEM. *p<0.05 vs. CA1 cells from estrus; $^{\&}$p<0.05 vs. DGGC from estrus; $^{\#}$p<0.05 vs. CA1 cells from diestrus.

Fig. 6. Characterization of AP potentiated $GABA_AR$ tonic currents in CA1PCs and DGGCs from hippocampal slices of adult female mice in the diestrus and estrus stages. A, (Upper panel) Morphology of CA1PC and DGGC recorded from hippocampal slice. Bar=10 µm. (Lower panel) Tonic current trace (I_{tonic}) recorded baseline, during 3 µM GABA (gray bar), and with 10 µM bicuculline (BIC, solid bar). Recordings in whole-cell mode, voltage-clamped at -60 mV. BIC decreased I_{tonic} and eliminated extrasynaptic currents. a: basal I_{tonic} (control); b: peak of GABA-enhanced I_{tonic}. B, Current traces expanded from panel *A* display baseline root-mean-square noise (I_{rms}) before application of GABA (control), in the presence of GABA alone (+GABA) or with BIC (+GABA + BIC). Note the larger I_{rms} in +GABA condition compared with the control and +BIC. C, Kolmogorov-Smirnov test was used to compare I_{rms} before and after application of GABA in DGGCs. I_{rms} in the presence of GABA (dotted line) was more than during baseline (solid line). D, Distribution of I_{rms} in the cell during the baseline period (open bars) and in the presence of GABA (black bars) The frequency distribution histogram demonstrates the rightward shift of I_{rms} in the presence of GABA in DGGC of diestrus. E, The

JPET Fast Forward. Published on May 10, 2013 as DOI: 10.1124/jpet.113.203653
This article has not been copyedited and formatted. The final version may differ from this version.

averaged tonic conductance (G_{tonic}, normalized I_{tonic} for cell capacitance, pS/pF, n = 4 - 12) and F, the averaged baseline noise conductance (G_{rms}, pS/pF). In the absence of GABA, G_{tonic} and G_{rms} were significantly higher in DGGC of diestrus than in estrus, whereas no difference was detected in CA1PCs. The G_{tonic} and G_{rms} peaks were enhanced in the presence of GABA application in all groups. G_{rms} was decreased in all conditions during BIC application. G, (Left panel) Representative current traces of tonic current activated by GABA (gray bar), potentiation by AP (light gray bar), and blocked by BIC (solid bar). (Right panel) Expansions from traces in the left panel display I_{rms} before application of GABA (control), in the presence of GABA alone (+GABA), with AP (+GABA + AP), and with BIC (+GABA + AP + BIC) from DGGC of diestrus. H, Summarized data of G_{tonic} and G_{rms} after application of AP in cells from DG and CA1 of diestrus (n=3-7). *p<0.05 vs. control within group; $^{\&}$p< 0.05 vs control at DGGC of diestrus group; $^{\#}$p< 0.05 vs. in the presence of GABA (+GABA).

Fig. 7. Ovarian cycle-related changes in susceptibility to hippocampus kindling epileptogenesis in mice. A, Rate of kindling epileptogenesis (number of stimulations required to induce stage 4/5 seizures) in control and allopregnanolone (AP, 3 mg/kg, s.c.)-treated animals at diestrus and estrus stages. AP was administered 15 min. before kindling session. B, Mean afterdischarge (AD) threshold values in mice at diestrus and estrus stages. C, Cumulative AD duration for the total time spent in electrographic seizure activity in control and AP-treated mice at diestrus and estrus stages. D, Representative traces of the electrographic afterdischarge seizure activity in control and AP-treated mice at diestrus and estrus stages. Traces show depth recordings from a right hippocampus stimulating/recording electrode. Arrows indicate onset of the 1 s kindling stimulus, which is followed by the stimulus artifact. Values represent mean ± SEM (n=6-9 mice per group.) *p<0.05; vs. estrus group; $^{\#}$p<0.05 vs. control diestrus group.

Fig. 8. Working model of ovarian cycle-related alterations of synaptic ($\alpha\beta\gamma$) and extrasynaptic ($\alpha\beta\delta$) $GABA_AR$ plasticity and function in the hippocampus. The diestrus stage is coupled with elevated progesterone, and consequently higher neurosteroid allopregnanolone levels in the brain. This promotes upregulation of neurosteroid-sensitive, extrasynaptic δ-subunit-containing $GABA_A$ receptor expression in the hippocampus dentate gyrus, which is a gateway for controlling hippocampus excitability. This molecular change could lead to increased tonic inhibition and thereby promote reduced susceptibility to seizures and other neurological conditions.

Figure-1

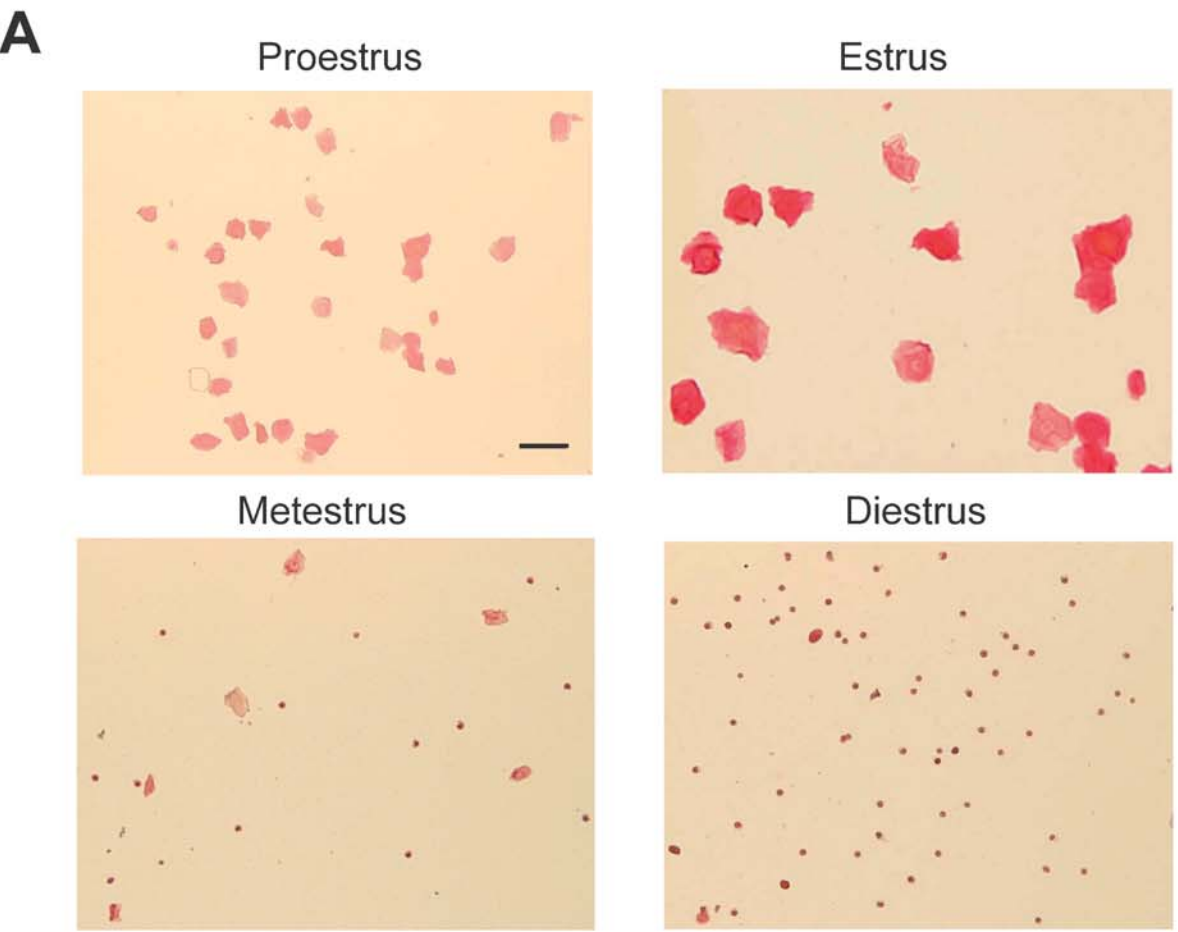

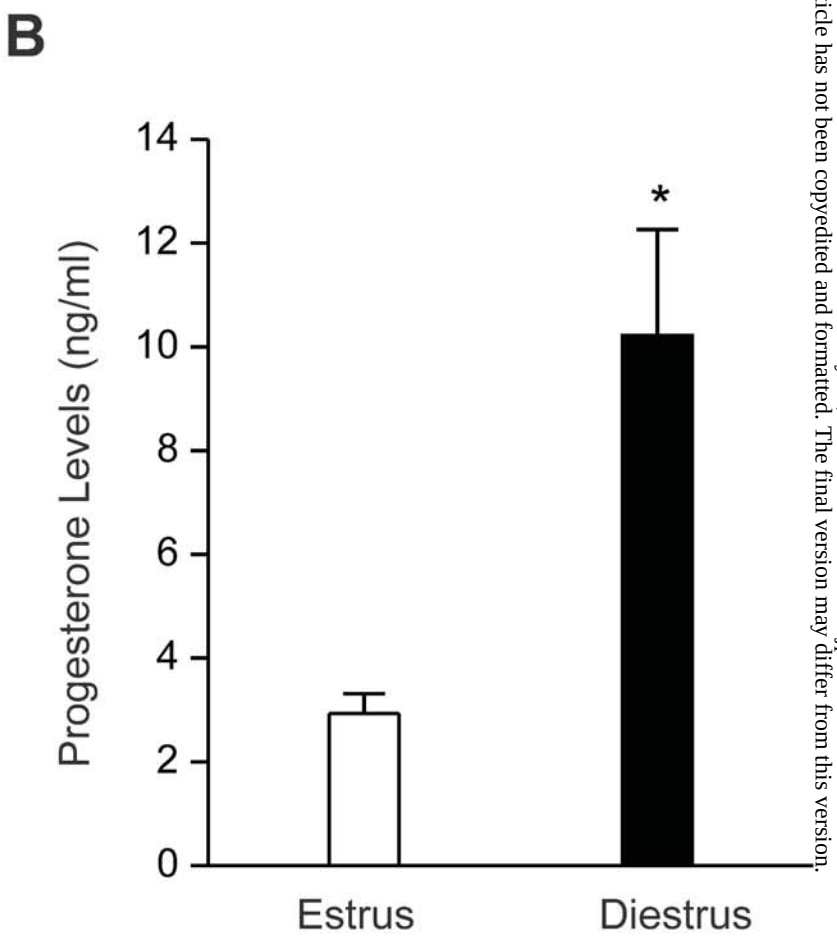

JPET Fast Forward. Published on May 10, 2013 as DOI: 10.1124/jpet.113.203653
This article has not been copyedited and formatted. The final version may differ from this version.

Figure-2

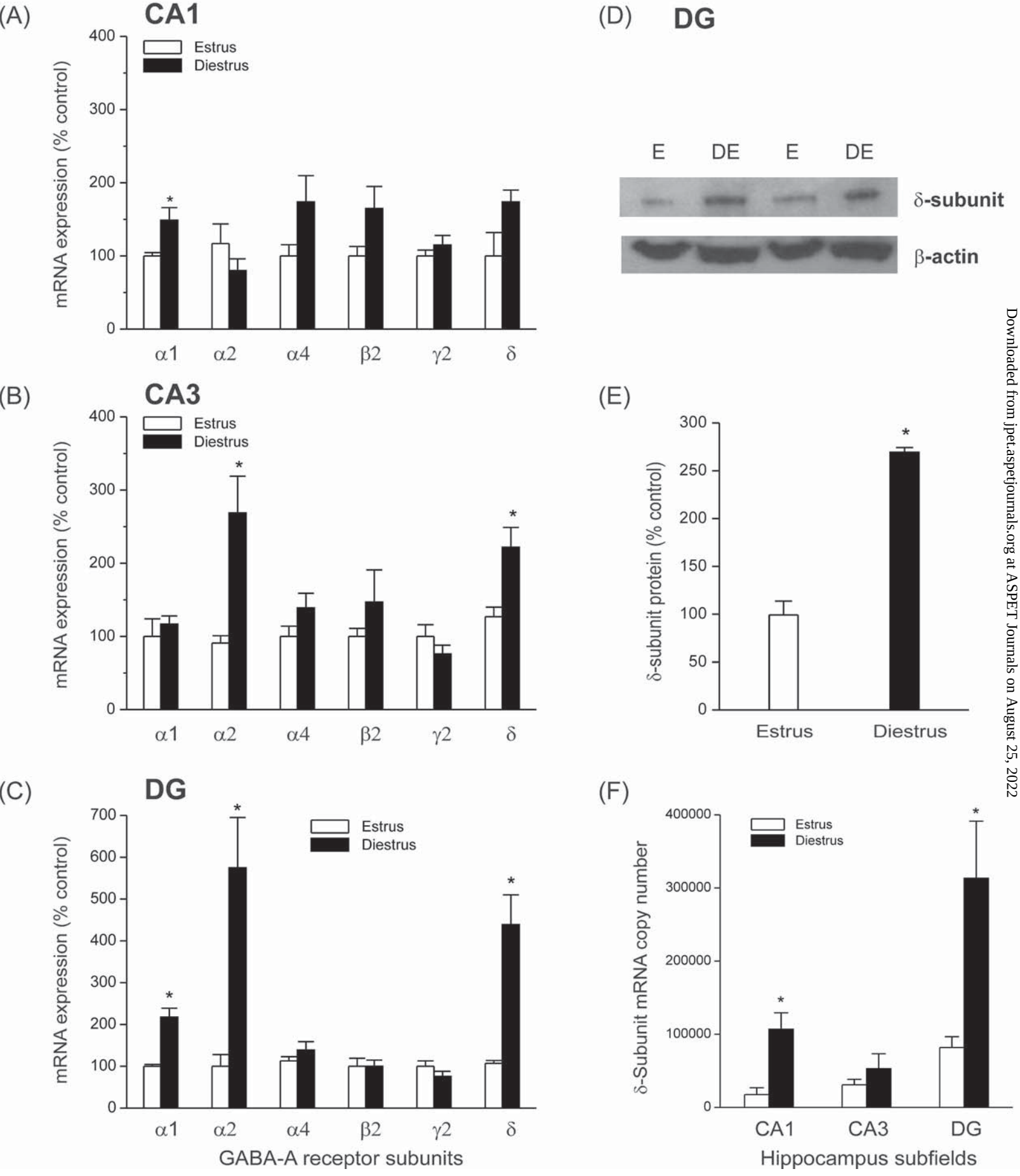

Figure-3

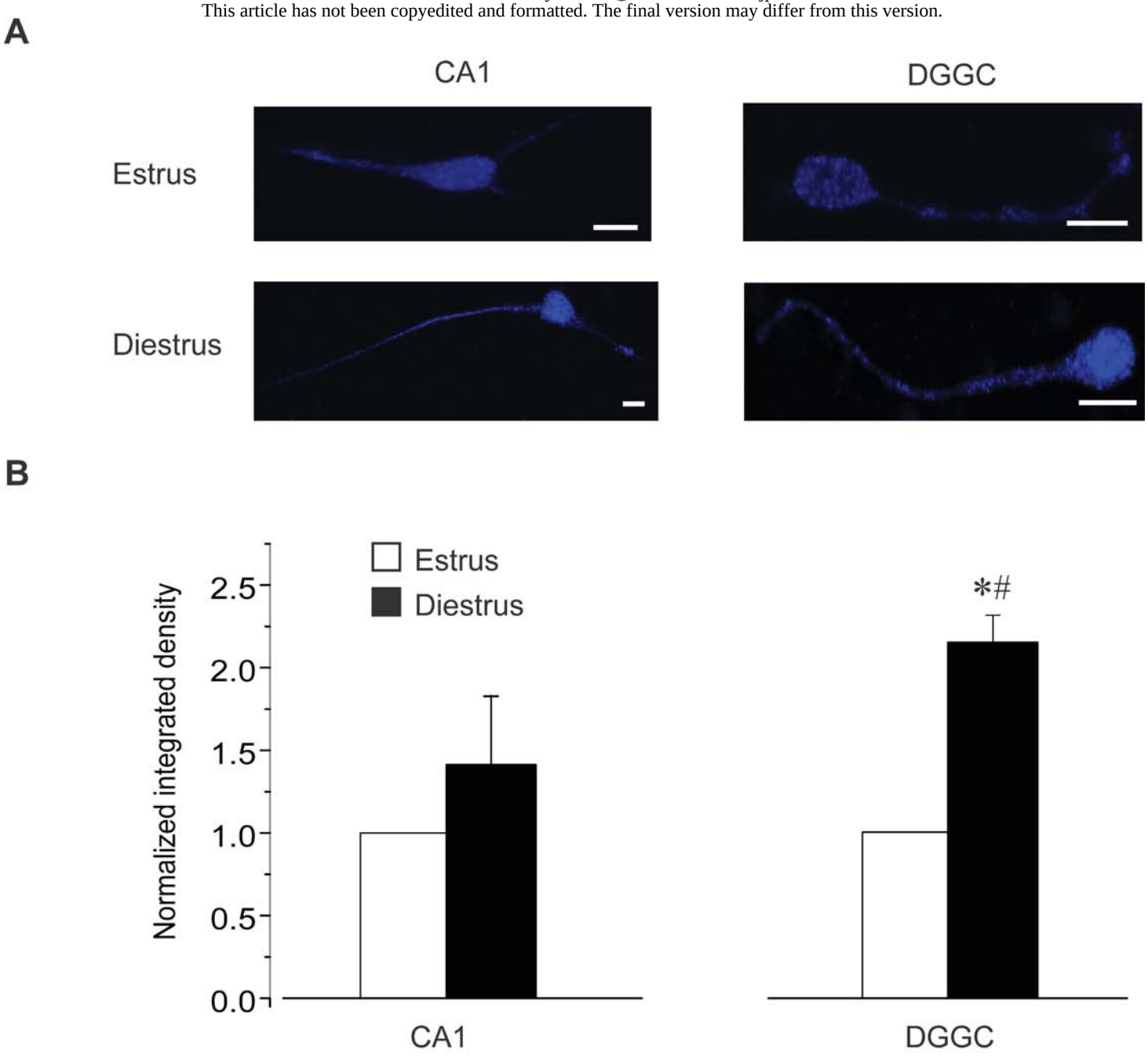

Figure-4

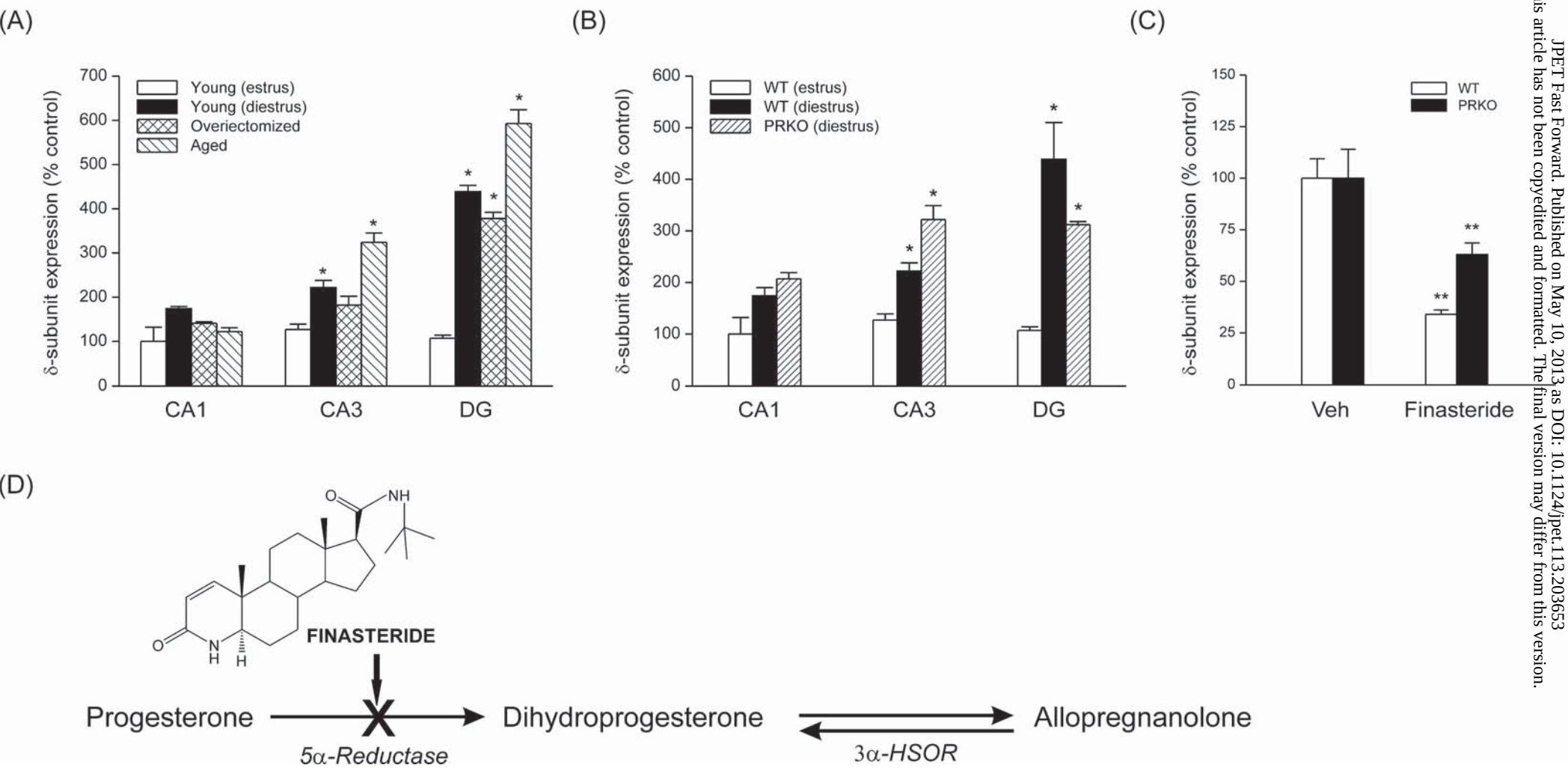

Figure-5

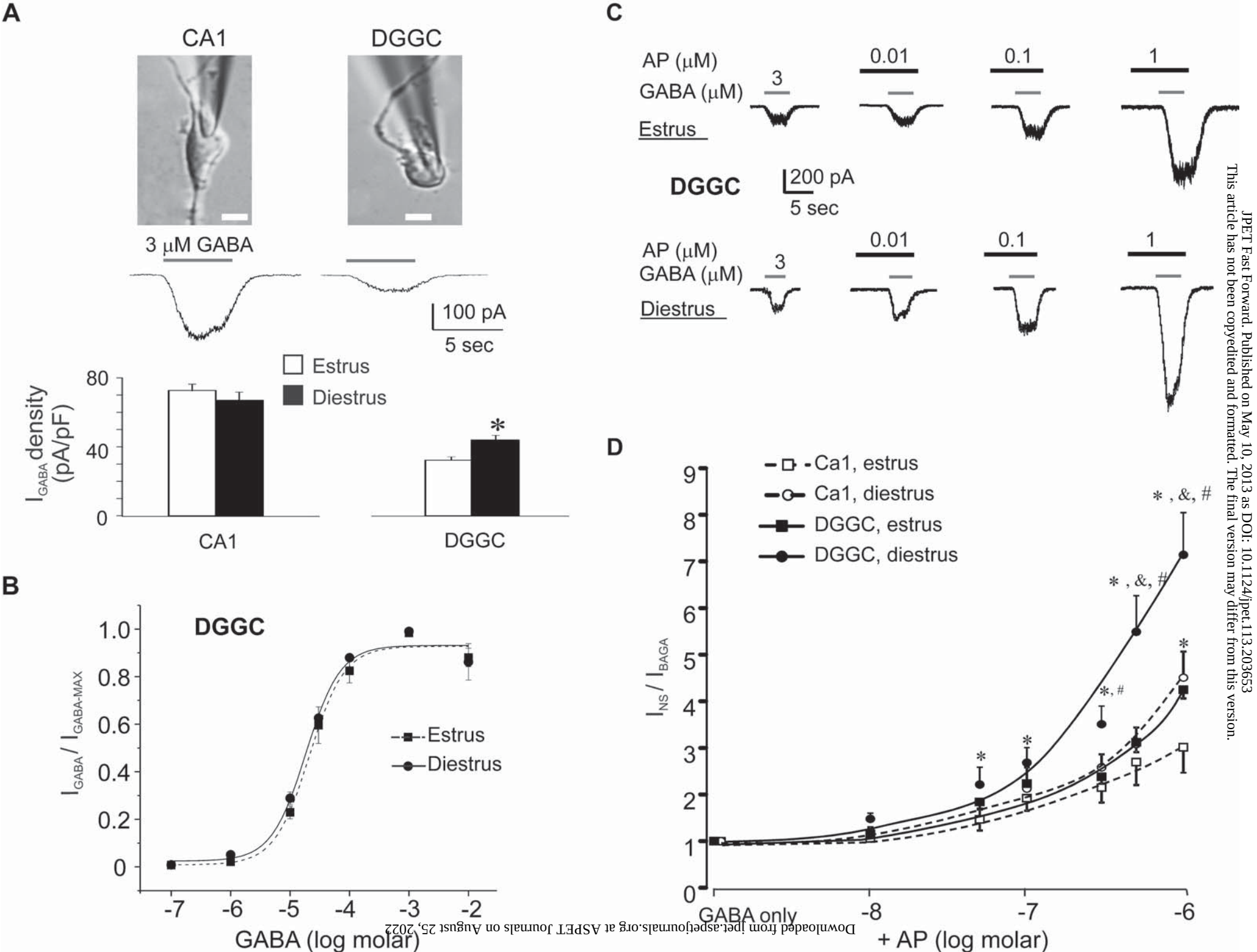

JPET Fast Forward. Published on May 10, 2013 as DOI: 10.1124/jpet.113.203653
This article has not been copyedited and formatted. The final version may differ from this version.

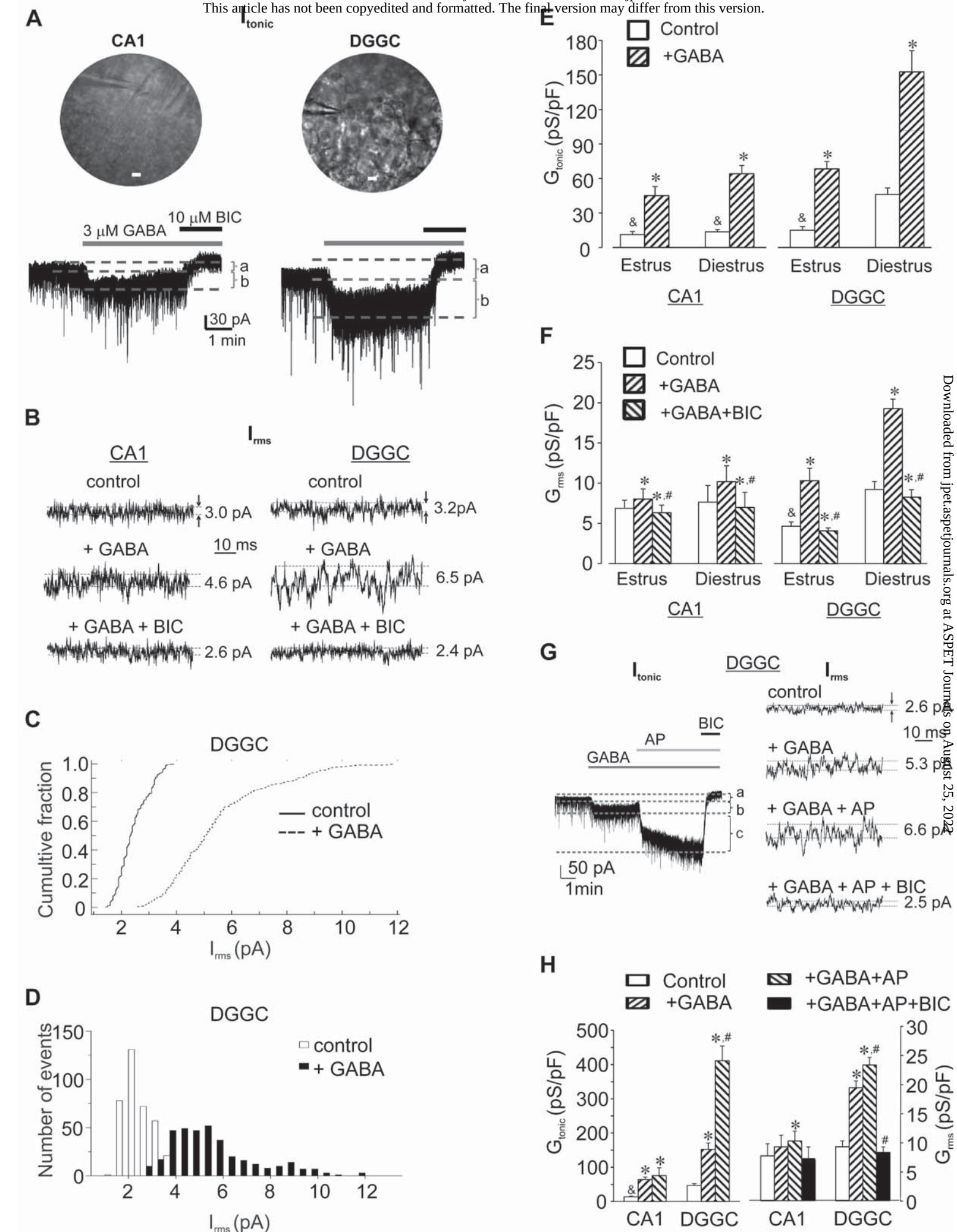

Figure-7

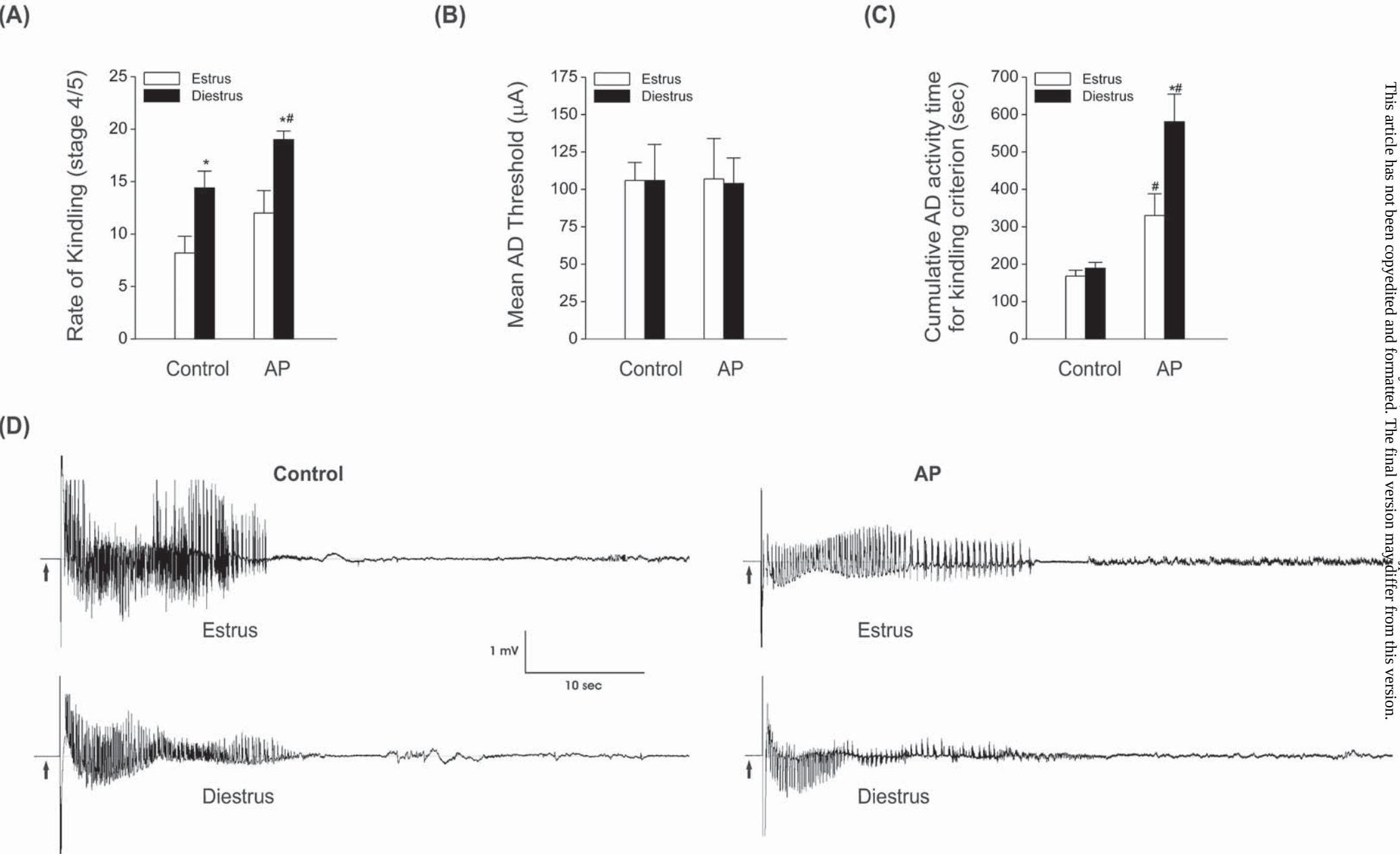

JPET Fast Forward. Published on May 10, 2013 as DOI: 10.1124/jpet.113.203653
This article has not been copyedited and formatted. The final version may differ from this version.

Figure-8